



**Luísa Maria Ramos Campelo**

Licenciatura em Biologia

**Fishing the key biological components of  
the bacterium *Geobacter metallireducens*  
for optimal biotechnological applications**

Dissertação para obtenção do Grau de Mestre em  
Biotecnologia

Orientador: Prof. Doutor Carlos A. Salgueiro, Professor Auxiliar,  
Faculdade de Ciências e Tecnologia, Universidade Nova de Lisboa

Júri:

Presidente: Prof. Doutora Paula M<sup>a</sup>. Theriaga M. B. Gonçalves

Arguente: Prof. Doutora Maria Teresa Nunes Mangas Catarino

Vogal: Prof. Doutor Carlos Alberto Gomes Salgueiro



FACULDADE DE  
CIÊNCIAS E TECNOLOGIA  
UNIVERSIDADE NOVA DE LISBOA

**02 Outubro, 2015**

**Luísa Maria Ramos Campelo**

Licenciatura em Biologia

**Fishing the key biological components of  
the bacterium *Geobacter metallireducens*  
for optimal biotechnological applications**

Dissertação para obtenção do Grau de Mestre em  
Biotecnologia

Orientador: Prof. Doutor Carlos A. Salgueiro, Professor Auxiliar,  
Faculdade de Ciências e Tecnologia, Universidade Nova de Lisboa

Júri:

Presidente: Prof. Doutor(a)

Arguente: Prof. Doutora Maria Teresa Nunes Mangas Catarino

Vogal(ais): Prof. Doutor Carlos Alberto Gomes Salgueiro



FACULDADE DE  
CIÊNCIAS E TECNOLOGIA  
UNIVERSIDADE NOVA DE LISBOA

**14 Setembro, 2015**



# Fishing the key biological components of the bacterium *Geobacter metallireducens* for optimal biotechnological applications

## “Copyright”

Luísa Maria Ramos Campelo

Faculdade de Ciências e Tecnologia  
Universidade Nova de Lisboa

Os resultados apresentados no capítulo 2 foram incluídos no artigo Dantas JM, Campelo LM, Duke NEC, Salgueiro CA, Pokkuluri PR (2015) "The structure of PccH from *Geobacter sulfurreducens* – a novel low reduction potential monoheme cytochrome essential for accepting electrons from an electrode", FEBS Journal, 282, 2215-2231.



Parte do trabalho experimental desta Dissertação foi realizado no âmbito do projecto de investigação científica, com referência PTDC/BBB-BEP/0753/2012”, financiado pela Fundação para a Ciência e a Tecnologia.

A Faculdade de Ciências e Tecnologia e a Universidade Nova de Lisboa têm o direito, perpétuo e sem limites geográficos, de arquivar e publicar esta dissertação através de exemplares impressos reproduzidos em papel ou de forma digital, ou por qualquer outro meio conhecido ou que venha a ser inventado, e de a divulgar através de repositórios científicos e de admitir a sua cópia e distribuição com objetivos educacionais ou de investigação, não comerciais, desde que seja dado crédito ao autor e editor.



## **Acknowledgements**

I would never have been able to finish my dissertation without the guidance of my advisor, Professor Carlos Salgueiro and Dr<sup>a</sup> Joana Dantas, help from friends, and support from my family.

Firstly, I would like to express my deepest gratitude to my advisor, Professor Carlos Salgueiro and Dr<sup>a</sup> Joana Dantas for their excellent guidance, caring, patience, and providing me with an excellent atmosphere for doing research.

Secondly, I would like to thank Telma Simões, who as a good friend, was always willing to help and give his best suggestions. It would have been a lonely lab without her. I thank my fellow labmates for the good mood.

Thirdly, I would also like to thank to my family, in especially to my mother. They were always supporting me and encouraging me with their best wishes.



## Abstract

The microorganisms from the *Geobacter* genus are very interesting because of their potential use for biotechnological applications. They can transfer electrons towards extracellular terminal acceptors, which include toxic or radioactive metals. In addition, they also have the capability to convert renewable biomass into electricity. The most studied members of the *Geobacter* genus are the *Geobacter metallireducens* and *Geobacter sulfurreducens* bacteria. *G. metallireducens* displays some particular physiological aspects that are even more interesting compared to *G. sulfurreducens*, which include (i) their ability to reduce aromatic compounds, (ii) more efficient Fe(III) reduction rates, and (iii) the ability to use nitrate as terminal electron acceptor. Similarly, to *G. sulfurreducens*, a family of five homologous periplasmic triheme *c*-type cytochromes, designated PpcA, PpcB, PpcC, PpcE and PpcF, was identified in *G. metallireducens*. In *G. sulfurreducens* the triheme cytochromes were shown to be crucial for extracellular electron transfer and therefore it is conceivable that these proteins play a similar role in *G. metallireducens*. Therefore, the main goal of this work was to optimize the production of *G. metallireducens* triheme cytochromes as a foundation to future optimization of *G. metallireducens*-based biotechnological applications. To achieve this goal, the proteins were cloned (except PpcB), heterologously expressed in *Escherichia coli* and purified. The preliminary characterization of PpcA and PpcF was also undertaken in the present work. The data obtained showed that both are low-spin hexacoordinated *c*-type cytochromes in the reduced and oxidized forms.

In parallel, it was also undertaken an evolutionary study on PccH, a monoheme *c*-type cytochrome from *G. sulfurreducens* that is crucial for microbial electrosynthesis pathways in this bacterium. The results obtained suggested that PccH is a member of a new subclass within the class I cytochromes.

**Keywords:** *Geobacter metallireducens*; *c*-type cytochrome; electron transfer; protein cloning, heterologous expression, protein purification





## Resumo

Os microorganismos do género *Geobacter* são muito interessantes devido ao seu potencial uso em aplicações biotecnológicas. A sua relevância deve-se à capacidade de transferir electrões para aceitadores extracelulares que incluem metais tóxicos ou radioactivos. Para além disso, conseguem ainda converter biomassa renovável em electricidade. As bactérias mais estudadas do género *Geobacter* são as das espécies *Geobacter metallireducens* e *Geobacter sulfurreducens*. Quando comparadas com *G. sulfurreducens*, as bactérias *G. metallireducens* apresentam alguns aspectos fisiológicos ainda mais interessantes e que incluem: (i) a capacidade de reduzir compostos aromáticos, (ii) uma maior eficiência na redução de Fe (III) e (iii) a capacidade de utilizar o nitrato como aceitador de electrões.

À semelhança de *G. sulfurreducens* foi possível identificar uma família composta por cinco citocromos tri-hémicos periplasmáticos do tipo *c* (designados por PpcA, PpcB, PpcC, PpcE e PpcF) em *G. metallireducens*. Em *G. sulfurreducens* os citocromos tri-hémicos periplasmáticos demonstraram ser cruciais para a transferência extracelular de electrões sendo por isso concebível estas proteínas desempenhem o mesmo papel em *G. metallireducens*.

O objetivo principal deste trabalho consistiu em otimizar a produção dos citocromos tri-hémicos de *G. metallireducens* tendo em vista uma futura optimização das aplicações biotecnológicas. Para atingir este objectivo estas proteínas foram clonadas (excepto o PpcB) e posteriormente expressas heterologamente em *Escherichia coli* e purificadas por técnicas cromatográficas. Foi ainda possível efectuar uma caracterização preliminar das propriedades dos citocromos PpcA e PpcF. Os resultados obtidos por espectroscopia de ressonância magnética nuclear e espectroscopia UV-visível indicam que ambas as proteínas se encontram no estado de *spin* baixo na forma oxidada e reduzida.

Paralelamente, também foi efectuado um estudo evolutivo sobre o citocromo *c* mono-hémico PccH de *G. sulfurreducens*, o qual se revelou crucial nas vias de electrossíntese desta bactéria. Os resultados obtidos mostram que este citocromo é um membro de uma nova sub-classe da classe I dos citocromos.

**Termos chave:** *Geobacter metallireducens*, citocromos do tipo *c*, transferência de electrões, Clonagem de proteínas, Expressão heteróloga, purificação de proteínas



## List of Contents

|  |       |
|--|-------|
| Acknowledgements.....  | v     |
| Abstract .....   | vii   |
| Resumo .....   | ix    |
| List of Contents.....  | xi    |
| List of Figures .....  | xiii  |
| List of tables.....  | xvi   |
| List of abbreviations and symbols.....   | xviii |
| 1. Chapter I.....  | 1     |
| 1.1. Introduction.....   | 3     |
| 1.1.1. <i>Geobacteraceae</i> .....   | 4     |
| 1.1.2. <i>Geobacter metallireducens</i> .....  | 5     |
| 1.1.3. c-type cytochromes .....  | 6     |
| 1.1.4. Periplasmic cytochromes <i>c</i> <sub>7</sub> in <i>Geobacter</i> .....                           | 7     |
| 1.2. Methods .....   | 11    |
| 1.2.1. Cloning of cytochromes <i>c</i> <sub>7</sub> from <i>G. metallireducens</i> .....                 | 13    |
| 1.2.2. Preparation of competent cell by the calcium chloride method .....                                | 15    |
| 1.2.3. Bacterial growth .....  | 15    |
| 1.2.4. Expression tests: PpcC and PpcE .....   | 16    |
| 1.2.5. Protein purification .....  | 16    |
| 1.2.6. NMR experiments .....   | 17    |
| 1.3. Results and discussion .....  | 19    |
| 1.3.1. Cloning of <i>c</i> <sub>7</sub> cytochromes from <i>G. metallireducens c</i> <sub>7</sub> .....  | 20    |
| 1.3.2. Heterologous expression of <i>c</i> <sub>7</sub> cytochromes from <i>G. metallireducens</i> ..... | 22    |
| 1.3.3. Protein purification and expression yields .....  | 23    |
| 1.3.4. Protein characterization.....   | 28    |
| 1.4. Future Work.....  | 31    |
| 2. Chapter II.....   | 33    |
| 2.1. Introduction .....  | 35    |
| 2.2. Methods.....  | 37    |
| 2.3. Results and Discussion .....  | 39    |
| 2.3.1. Comparison with other monoheme cytochromes .....  | 40    |
| 3. References.....   | 45    |
| 4. Supplementary .....   | 49    |
| 4.1. Cloning.....  | 51    |
| A. Primers design.....   | 52    |
| B. PCR programs.....   | 54    |
| C. Gel electrophoresis .....   | 55    |
| D. DNA Sequencing Results.....   | 57    |

|  |    |
|--|----|
| 4.2. Purification .....                                    | 59 |
| E. PpcF purification steps.....                            | 60 |
| F. Purification of PpcC .....                              | 61 |
| G. Purification of PpcE.....                               | 63 |
| H. Resume of Purification .....                            | 65 |
| 4.3. Spectrometry and Spectroscopic Characterization ..... | 67 |
| I. Mass spectrometry spectra .....                         | 68 |
| J. Visible spectra .....                                   | 69 |
| K. NMR spectra.....  | 71 |
| L. Solutions.....  | 72 |

## List of Figures

|   |    |
|---|----|
| <b>Figure 1:</b> Scheme of a <i>Geobacter</i> -powered microbial fuel cell.....   | 5  |
| <b>Figure 2:</b> The structure of <i>c</i> -type heme group labelled accordingly to the IUPAC nomenclature.6  | 6  |
| <b>Figure 3:</b> Structures of triheme periplasmic cytochromes from <i>Geobacter sulfurreducens</i> : PpcA, PpcB, PpcC, PpcD and PpcE.....  | 7  |
| <b>Figure 4:</b> The <i>nar</i> operon encodes the nitrate and nitrite transporters ( <i>narK</i> -1, <i>narK</i> -2), two <i>c</i> -type cytochromes including PpcF, and two genes of molybdenum cofactor biosynthesis ( <i>moaA</i> -2, <i>moaA</i> -2) .....   | 8  |
| <b>Figure 5:</b> Alignment of cytochromes <i>c</i> <sub>7</sub> amino acid sequences .....  | 9  |
| <b>Figure 6:</b> Overview of the methodology used to clone, produce, purify and characterize triheme cytochromes from <i>G. metallireducens</i> .....   | 12 |
| <b>Figure 7:</b> Gel electrophoresis 0.8% to evaluate the quality of PCR fragments. ....  | 20 |
| <b>Figure 8:</b> Gel electrophoresis 0.8% resulting from PCR of colonies of PpcA.....   | 21 |
| <b>Figure 9:</b> A - Plasmid pCSGmet2902-PpcA resulting from the cloning of PpcA sequence. B - Plasmid pCSGmet3165-PpcC resulting from the cloning of PpcC sequence. C - Plasmid pCSGmet3166-PpcE resulting from the cloning of PpcC sequence. D - Plasmid pCSGmet0335-PpcF resulting from the cloning of PpcC sequence. In each plasmid, the arrows indicate the hybridization site of pCK32 primers. .... | 21 |
| <b>Figure 10:</b> Pellets from periplasmic fraction of PpcF and PpcE. ....  | 22 |
| <b>Figure 11:</b> SDS-PAGE electrophoresis gel stained with Coomassie blue and TMBZ/H <sub>2</sub> O <sub>2</sub> for the periplasmic fractions of PpcE obtained from cell cultures induced with different concentrations of IPTG.....  | 22 |
| <b>Figure 12:</b> SDS-PAGE electrophoresis gel stained with Coomassie blue and TMBZ/H <sub>2</sub> O <sub>2</sub> for the periplasmic fractions of PpcC obtained from cell cultures induced with different concentrations of IPTG. ....   | 23 |
| <b>Figure 13:</b> Elution profile for the cation exchange column chromatography equilibrated with 10 mM Tris-HCl, pH 8 (flow rate of 1 ml/min) for PpcA.....  | 24 |
| <b>Figure 14:</b> SDS-PAGE electrophoresis gel stained with Coomassie blue and TMBZ/H <sub>2</sub> O <sub>2</sub> for the main peaks obtained in the chromatographic purification steps of PpcA.....  | 24 |
| <b>Figure 15:</b> Elution profile for the molecular exclusion column chromatography equilibrated with 100 mM sodium phosphate buffer, pH 8 for PpcA.....  | 25 |
| <b>Figure 16:</b> A- Elution profile for the cation exchange column chromatography equilibrated with 10 mM Tris-HCl, pH 8 for PpcF (flow rate of 1 ml/min). B- SDS-PAGE electrophoresis gel stained with Coomassie blue from the collected fractions during the cation exchange column chromatography.....  | 25 |
| <b>Figure 17:</b> Elution profile obtained in molecular exclusion column chromatography for each band obtained in the cationic exchange chromatography step for PpcF.. ....   | 26 |
| <b>Figure 18:</b> SDS-PAGE electrophoresis gel stained with Coomassie Blue correspondent to the fractions of the more intense band obtained in the molecular exclusion chromatography of PpcF purification procedure.....   | 27 |
| <b>Figure 19:</b> Visible absorption spectra of PpcA in the oxidized and reduced forms.....   | 28 |
| <b>Figure 20:</b> 1D- <sup>1</sup> H NMR spectra of PpcA (70 μM) obtained at 25 °C before and after lyophilization.....   | 29 |
| <b>Figure 21:</b> 1D- <sup>1</sup> H NMR spectra of the reduced and oxidized triheme cytochrome PpcA (70 μM) obtained at 25 °C, pH 8. The typical regions of the heme substituents in the oxidized spectrum are indicated. ....   | 30 |

|   |    |
|---|----|
| <b>Figure 22:</b> Sequence alignment of the top six hits returned for the amino acid sequence of the mature PccH using the basic local alignment search tool (BLAST).....   | 40 |
| <b>Figure 23:</b> Amino acid sequence comparison of Gs PccH cytochrome c with prokaryotic c-type monoheme cytochromes. ....   | 41 |
| <b>Figure 24:</b> A gallery of representative bacterial class I monoheme cytochromes including PccH shown as cartoons. ....   | 43 |
| <b>Figure A- 1:</b> Sequence of <i>ppcA</i> and the primers forward and reverse used for the gene amplification.....  | 52 |
| <b>Figure A- 2:</b> Sequence of <i>ppcC</i> and the primers forward and reverse used for the gene amplification.....  | 52 |
| <b>Figure A- 3:</b> Sequence of <i>ppcE</i> and the primers forward and reverse used for the gene amplification.....  | 53 |
| <b>Figure A- 4:</b> Sequence of <i>ppcF</i> and the primers forward and reverse used for the gene amplification.....  | 53 |
| <b>Figure C- 1:</b> Agarose gel electrophoresis (0.8%) with the result of PCR fragment amplification for <i>ppcC</i> (351 bp), <i>ppcE</i> (336 bp), <i>ppcB</i> (336 bp).....                                      | 55 |
| <b>Figure C- 2:</b> Agarose gel electrophoresis (0.8%) with the result of colonies PCR amplification with pCK32 primers for PpcB and PpcC. ....   | 55 |
| <b>Figure C- 3:</b> Agarose gel electrophoresis (0.8%) with the result of colonies PCR amplification with pCK32 primers for PpcC and PpcE. ....   | 55 |
| <b>Figure C- 4:</b> Agarose gel electrophoresis (0.8%) with the result of PCR fragment amplification for <i>ppcB</i> (336 bp) with a different cloning protocol described in section 1.3.1.....                     | 56 |
| <b>Figure D- 1:</b> DNA sequencing results for each c-type cytochrome from <i>G. metallireducens</i> . ....   | 57 |
| <b>Figure E- 1:</b> Elution profile for the cation exchange column chromatography equilibrated with 10 mM Tris-HCl, pH 7.5 (flow rate of 1 ml/min) for PpcF.....  | 60 |
| <b>Figure E- 2:</b> Elution profile for the cation exchange column chromatography equilibrated with 10 mM Tris-HCl, pH 8.5 (flow rate of 1 ml/min) for PpcF.....  | 60 |
| <b>Figure F- 1:</b> Elution profile for the cation exchange column chromatography equilibrated with 10 mM Tris-HCl, pH 8 for PpcC.....  | 61 |
| <b>Figure F- 2:</b> Elution profile for the molecular exclusion column chromatography equilibrated with 100 mM sodium phosphate buffer, pH 8 for PpcC.....  | 61 |
| <b>Figure F- 3:</b> SDS-PAGE electrophoresis gel stained with Comassie blue (A) and the TMBZ/H <sub>2</sub> O <sub>2</sub> (B) correspondent to the collected fractions of PpcC cytochrome purification steps ..... | 62 |
| <b>Figure G- 1:</b> Elution profile for the cation exchange column chromatography equilibrated with 10 mM Tris-HCl, pH 8 for PpcE .....   | 63 |
| <b>Figure G- 2:</b> Elution profiles for the molecular exclusion column chromatography equilibrated with 100 mM sodium phosphate buffer, pH 8 for PpcE.....   | 63 |
| <b>Figure G- 3:</b> SDS-PAGE electrophoresis gel stained with Comassie blue (A) and the TMBZ/H <sub>2</sub> O <sub>2</sub> (B) correspondent to the collected fractions of PpcE cytochrome purification steps ..... | 64 |
| <b>Figure I- 1:</b> Mass spectrometry spectrum of purified PpcA .....   | 68 |
| <b>Figure I- 2:</b> Mass spectrometry spectrum of purified PpcF.....  | 68 |
| <b>Figure J- 1:</b> Absorption spectrum of PpcF in the oxidized and reduced .....   | 69 |
| <b>Figure J- 2:</b> Absorption spectrum of PpcC in the oxidized and reduced.....  | 69 |
| <b>Figure J- 3:</b> Absorption spectrum of PpcE in the oxidized and reduced. ....   | 70 |

**Figure K- 1:** 1D-<sup>1</sup>H NMR spectra of the oxidized before and after lyophilized triheme cytochrome PpcF (70 μM) obtained at 25 °C. ....71

**Figure K- 2:** 1D-<sup>1</sup>H NMR spectra of the reduced and oxidized triheme cytochrome PpcF (70 μM) obtained at 25 °C. ....71



## List of tables

|   |    |
|---|----|
| <b>Table 1:</b> Access number in Kyoto Encyclopedia of Genes and Genomes Web site and signal peptide cleavage site calculated by two bioinformatics tools for the five periplasmic triheme cytochromes from <i>G. metallireducens</i> ..... | 13 |
| <b>Table 2:</b> Primers used to amplify the sequence of each protein. ....  | 14 |
| <b>Table 3:</b> Expression yields for triheme cytochromes from <i>G. metallireducens</i> . ....   | 27 |
| <b>Table 4:</b> Summary of the optical absorption maxima in oxidized and reduced spectra for each triheme cytochrome from <i>G. metallireducens</i> . ....  | 29 |
| <b>Table B- 1:</b> PHUSION program.....   | 54 |
| <b>Table B- 2:</b> PCR colonies program .....   | 54 |
| <b>Table H- 1:</b> Calculated molecular weight and isoelectric point for the triheme cytochromes from <i>G. metallireducens</i> using the EXPASY tool.....  | 65 |
| <b>Table H- 2:</b> Elution gradient value and elution volume for the triheme cytochromes from <i>G. metallireducens</i> in the cationic and molecular exclusion chromatography steps, respectively...                                       | 65 |
| <b>Table L- 1:</b> Main solutions used in this work.....  | 71 |
| <b>Table L- 2:</b> Heme dye solution protocol.....  | 72 |



## List of abbreviations and symbols

|                   |   |
|-------------------|---|
| 1D                | One dimensional   |
| 2D                | Two dimensional   |
| 2xYT              | 2x yeast extract-tryptone medium                          |
| AQDS              | Anthraquinone-2,6-disulfonic acid                         |
| AMP               | Ampicillin  |
| BCA               | Bicinchoninic acid assay                                  |
| BLAST             | Basic local alignment search tool                         |
| CLO               | Chloramphenicol   |
| DNA               | Deoxyribonucleic acid                                     |
| D <sub>2</sub> O  | Deuterium oxide (heavy water)                             |
| <i>E.coli</i>     | <i>Escherichia coli</i>                                   |
| EDTA              | Ethylenediamine tetra-acetic acid                         |
| IPTG              | Isopropyl β-D-1-thiogalactopyranoside                     |
| LB                | Luria Broth medium  |
| NCBI              | National center for biotechnology information             |
| MW                | Molecular weight  |
| NaPi              | Sodium phosphate buffer                                   |
| NMR               | Nuclear magnetic Resonance                                |
| NOESY             | Nuclear Overhauser effect spectroscopy                    |
| OD <sub>600</sub> | Optical density at 600 nm                                 |
| pI                | Isoelectric point   |
| ppm               | Parts per million   |
| PSA               | Persulfate ammonium                                       |
| rpm               | Rotations per minute                                      |
| SDS-PAGE          | Sodium dodecyl sulfate polyacrylamide gel electrophoresis |
| TEMED             | Tetramethylethylenediamine                                |
| Tris              | Tris(hydroxymethyl)aminomethane                           |
| TOCSY             | Total correlation spectroscopy                            |
| UV-visible        | Ultraviolet-visible                                       |
| ε <sub>552</sub>  | Absorption extinction coefficient at 552 nm               |

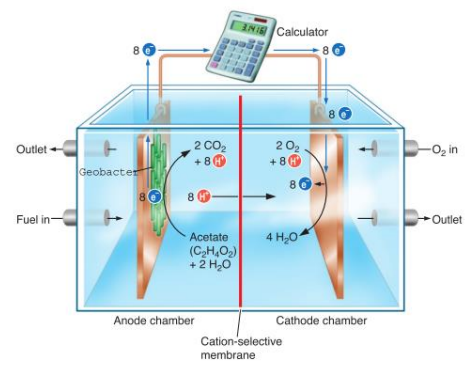


# 1. Chapter I

Fishing the key biological components of the bacterium *Geobacter metallireducens* for optimal biotechnological applications



# 1.1. Introduction



### 1.1.1. *Geobacteraceae*

The *Geobacter* genus represents one of the most usually studied groups of microorganisms capable of extracellular electron exchange. It is characterized by Gram-negative and anaerobic bacteria from the  $\delta$ -Proteobacteria family. However, recently, studies suggested that *Geobacter sulfurreducens* can tolerate small amounts of oxygen and are therefore not strictly anaerobic<sup>1</sup>. The members of *Geobacter* genus are commonly found in several environments due to their important role in degradation of organic compounds and bioremediation of toxic metals, especially in aquifers polluted by or rich in organic matter<sup>2-5</sup>. These bacteria are particularly abundant in Fe(III) rich environments in which they promote the metal reduction process. Therefore, it is fundamental to understand the environmental factors that modulate their growth and metabolic activity<sup>6</sup>.

The *Geobacter* members are very interesting due to their roles in the carbon and metal cycles in the aquatic sediments. They are relevant from the point of view of bioremediation in underground aquifers contaminated by organic and metal compounds as mentioned above. The *Geobacter* group can be also used in microbial fuel cells (MFCs) for producing electricity from organic matter in which microorganisms are the catalyst for oxidizing the organic matter (**Figure 1**). The anaerobic anode chamber contains organic fuel and a graphite electrode. The cathode chamber has a similar electrode and is aerobic. *Geobacter* transfers electrons released from the oxidation of organic matter onto the anode. The electrons flow from the anode to the cathode. The two chambers are separated by a cation-selective membrane that permits the protons that are released from oxidized organic matter to migrate to the cathode side, where they combine with electrons and oxygen to form water<sup>6</sup>. However, difficulties in scaling up MFCs for extracting energy on an industrial scale have significantly limited their short-term practical use<sup>7</sup>.

In 1987, *Geobacter metallireducens* was the first microorganism to be isolated from sediments in the Potomac River from Washington D.C. This bacteria obtains its metabolic energy by using iron oxide in the same way that humans use oxygen. *G. metallireducens* and other species that have subsequently been isolated from a wide diversity of environments represent a very important model of iron transformations on modern earth and may explain geological phenomena, such as the massive accumulation of magnetite in ancient iron formations<sup>8</sup>.

The most studied members of the *Geobacteraceae* family are the *G. sulfurreducens* and *G. metallireducens*. The first studies on the mechanisms for Fe (III) oxide reduction were carried out on *G. sulfurreducens* because it was the first species of this family for which a genetic system was developed<sup>9</sup>. *G. metallireducens* is a more effective Fe (III) oxide reducer than *G. sulfurreducens* it shows other particular physiological features<sup>10</sup>. In fact, in contrast with *G. sulfurreducens*, *G. metallireducens* do not use fumarate as a final electron acceptor. To date, nitrate is the only non-metallic electron acceptor that can be used by these bacteria, besides anthraquinone-2,6-disulfonic acid (AQDS) and humics<sup>6</sup>.



Nowadays, *G. metallireducens* is more appealing than *G. sulfurreducens* in some physiological aspects, which include for example aromatic compounds metabolization<sup>11</sup>.

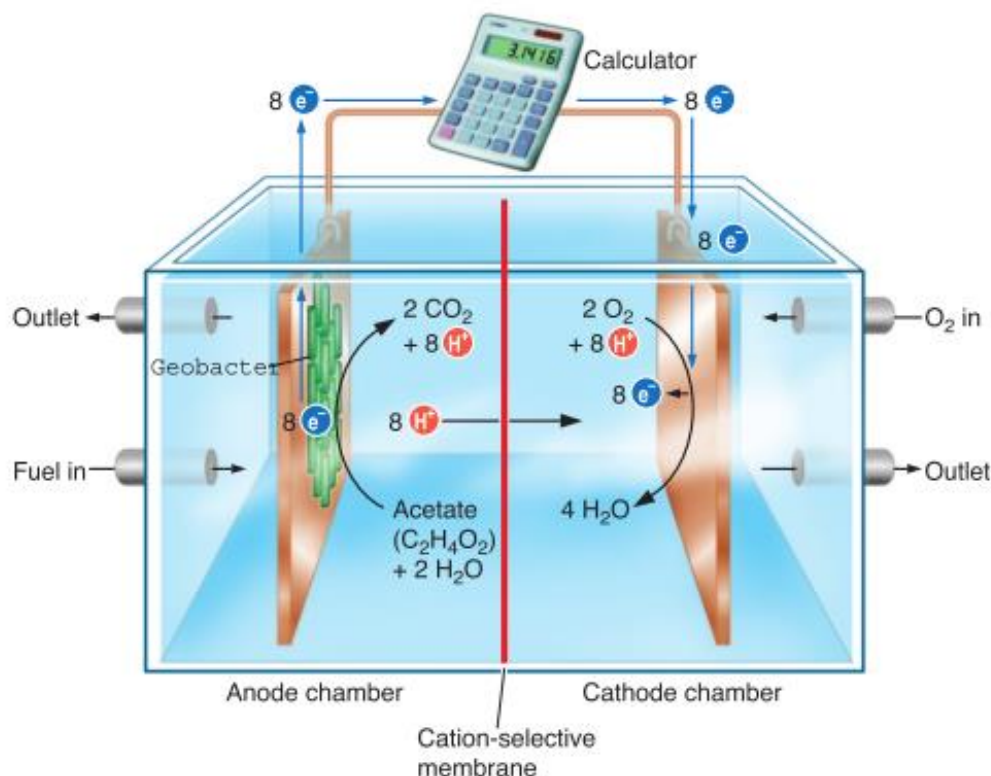


**Figure 1: Scheme of a *Geobacter*-powered microbial fuel cell<sup>12</sup>.** The anaerobic anode chamber contains the organic fuel, whereas the cathode chamber is aerobic. *Geobacter* cells transfer electrons released from the oxidation of the organic fuel onto the anode, which can be used to power electric devices. The two chambers are separated by a cation-selective membrane that permits the protons that are released to migrate to the cathode side, where they combine with electrons and oxygen to form water.

### 1.1.2. *Geobacter metallireducens*

*G. metallireducens* has a high importance since it was the first discovered microorganism with the ability to: (i) storage energy for their own growth from the oxidation of compounds coupled to reduction of Fe(III), Mn(IV) or U(VI); (ii) oxidize aromatic hydrocarbons under anaerobic conditions<sup>13</sup>; (iii) utilize humic substances as electron acceptors; (iv) couple the oxidation of organic compounds to carbon dioxide using an electrode as the sole electron acceptor and (v) use of a poised electrode as a direct electron donor<sup>10</sup>

As mentioned above, *G. metallireducens* is a dissimilatory iron reducing bacterium that also has the ability to respire nitrate to ammonia. In this process, the biochemical characterization of its components revealed that c-type cytochromes appear to be over-expressed when the cells utilize nitrate as terminal electron acceptor. In previous studies, a cytochrome c-containing enzyme complex that exhibits both nitrate and nitrite reductase activities has been described<sup>14</sup>.

Tremblay and co-workers<sup>15</sup> identify a very important role for *pilli* in the Fe(III) reduction and in the transfer of electrons to electrodes in *G. metallireducens*. The motility is one of the reasons why these bacteria are more efficient in the reduction of Fe (III) oxides compared to *G. sulfurreducens*. However the *c*-type cytochromes are important to this process as well<sup>15</sup>. To date, the components and mechanisms underlying the extracellular electron transfer in *G. metallireducens* are not yet fully elucidated<sup>16</sup>. This is a crucial step to contribute to develop future applications in biofuel production and bioremediation.

### 1.1.3. C-type cytochromes

Despite the lack of information regarding the precise extracellular electron transfer mechanisms, it is consensual that *c*-type cytochromes play a crucial role in this process. Cytochromes are electron transfer proteins containing one or more heme groups. The heme group is formed by a tetrapyrrole porphyrin ring coordinated to an iron atom. The cytochromes have characteristic absorption bands in the visible wavelength range that change with redox, spin and coordination state. Cytochromes can be classified as type *a*, *b*, *c* or *d* according to the type of substituents at the periphery of the porphyrin ring<sup>17</sup>.

The small size, high solubility and high helical content and the presence of the heme cofactor have permitted the study of cytochromes *c* through a variety of spectroscopic techniques<sup>18</sup>. In *c*-type cytochromes the heme(s) group(s) is covalently bound through thioether bonds to cysteine residues of the polypeptide chain arranged in a typical CXXCH motif<sup>17</sup>. The heme group (**Figure 2**) is composed by proton-containing groups (four methyl groups, four meso protons, two thioether protons, two thioether methyl and two propionate groups)<sup>19</sup>.

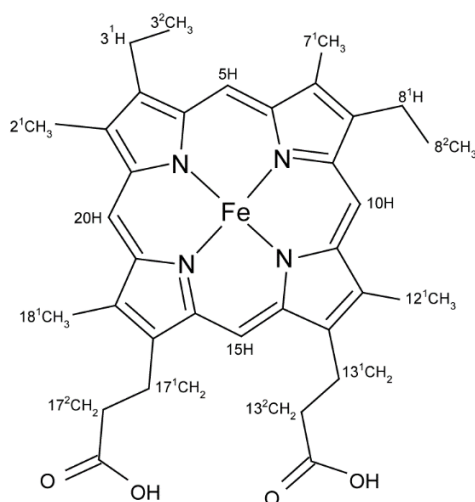


**Figure 2: The structure of *c*-type heme group labelled accordingly to the IUPAC nomenclature<sup>19</sup>.** The two thioether bonds (not shown) are established between atoms 3<sup>1</sup>H and 8<sup>1</sup>H with the sulfur atom of the cysteine residues in the heme binding motif.

#### 1.1.4. Periplasmic cytochromes $c_7$ in *Geobacter*

Some extracellular electron transport components are well conserved between *G. sulfurreducens* and *G. metallireducens*. This is the case of the genes coding the MacA (Gmet\_3091 and GSU\_0445) and PpcA (Gmet\_2902 and GSU\_0612), which are involved in Fe (III) and U(VI) reduction. However many of the genes that code for extracellular electron transfer by *G. sulfurreducens*, like some essential *c*-type cytochromes, don't have homologs in *G. metallireducens*.

Five triheme periplasmic cytochromes, designated PpcA, PpcB, PpcC, PpcD and PpcE, were identified in *G. sulfurreducens*<sup>22, 23</sup>. These five cytochromes are small soluble proteins, each with approximately 10 kDa<sup>20</sup>, and have been extensively studied. These cytochromes have bis-His axial coordination, different and negative redox potentials and their structures have been determined<sup>22</sup> (**Figure 3**). The hemes are numbered I, III and IV, a designation that derives from the superimposition of the hemes with those of the structurally homologous tetraheme cytochromes  $c_3$ .<sup>22-24</sup>

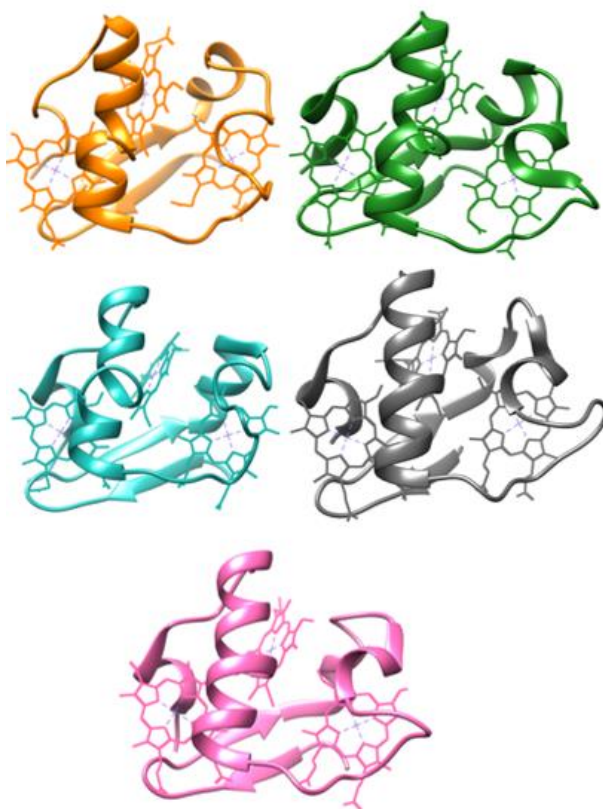


**Figure 3: Structures of triheme periplasmic cytochromes from *Geobacter sulfurreducens*: PpcA (2LDO, orange), PpcB (3BXU, green), PpcC (3H33, blue), PpcD (3H4N, grey) and PpcE (3H34, pink). PDB accession code in parenthesis with the corresponded color in the figure.**

Similarly, it was also possible to identify a family of five triheme periplasmic cytochromes in *G. metallireducens*, PpcA, PpcB, PpcC, PpcE and PpcF. The designation for

cytochrome PpcF derives from the the relative little homology of this protein with PpcD. As mentioned above, it is suggested that these triheme cytochromes are involved in extracellular electron exchange. In particular, PpcA (coded by gene *gmet2902*) was shown to be important for direct interspecies electron transfer (DIET). DIET consists in microbial syntrophy in which microorganisms establish electrical connections for the transfer of electrons from one syntrophic partner to another<sup>7</sup>. PpcA doesn't directly help to make extracellular electrical contact between the microorganisms, though it is involved in the process of extracellular electron transfer<sup>25</sup>.

On the other hand PpcF (coded by gene *Gmet0335*) allows the transfer of electrons to the nitrate reductase from extracellular electron donors such as humic substances or graphite electrodes<sup>10</sup>. As mentioned above, *G. metallireducens* has the ability to reduce nitrate, in contrast with *G. sulfurreducens*. The nitrate reductase activity of *G. metallireducens* is attributed to the *narGYJl* genes (**Figure 4**). The gene *ppcF* of *nar* operon encodes a periplasmic triheme c-type cytochrome involved in this reduction processes.

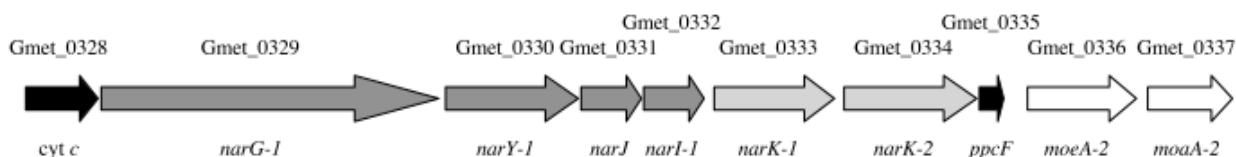


**Figure 4: The *nar* operon encodes the nitrate and nitrite transporters (*narK-1*, *narK-2*), two c-type cytochromes including PpcF, and two genes of molybdenum cofactor biosynthesis (*moeA-2*, *moaA-2*)<sup>10</sup>.**

Using the PpcF amino acid sequence, the non-redundant amino acid database of NCBI was searched using the Basic Local Alignment Search Tool (Blast)<sup>26</sup>, and in addition to the five cytochromes *c<sub>7</sub>* mentioned above, other cytochromes *c<sub>7</sub>* were found: *Geobacter metallireducens*; *Geobacter sulfurreducens* KN400; *Geobacter sulfurreducens* PCA; *Geobacter sp.* M18; *Geobacter bemidjensis*; *Geobacter lovleyi*; *Pelobacter propionicus*. (**Figure 5**).

This work constitutes the first step to understand the role of periplasmic triheme cytochromes in *G. metallireducens* and simultaneously build foundations to optimize future biotechnological applications driven by these bacteria. In order to achieve this goal it is first necessary to clone, express and purify each protein (PpcA, PpcB, PpcC, PpcE and PpcF).

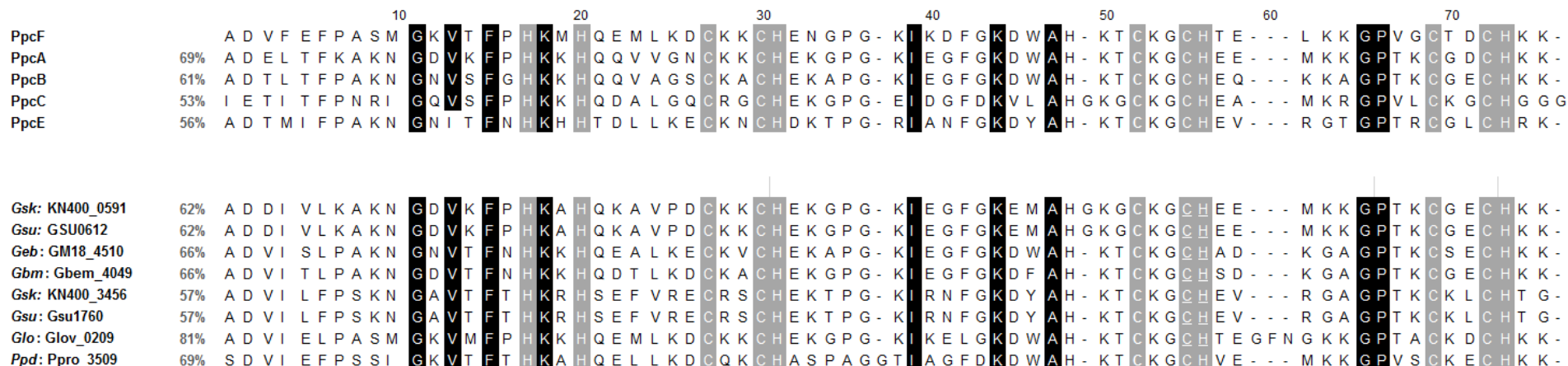
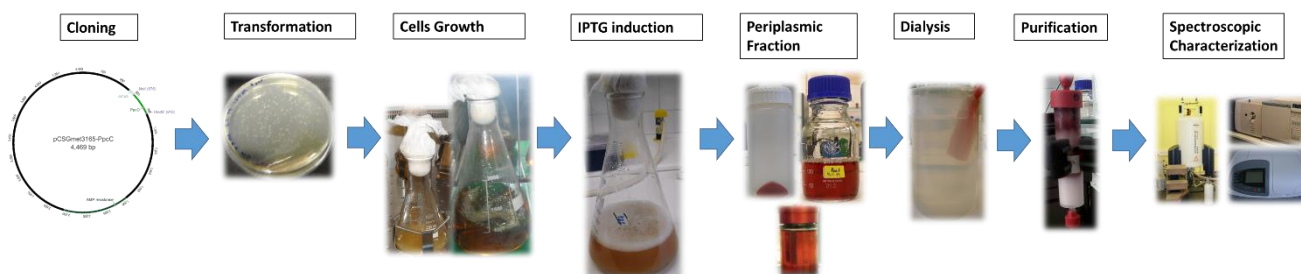


**Figure 5: Alignment of cytochromes  $c_7$  amino acid sequences.** PpcA-F, *Geobacter metallireducens*; Gsk, *Geobacter sulfurreducens* KN400; Gsu, *Geobacter sulfurreducens* PCA; Geb, *Geobacter* sp. M18; Gbm, *Geobacter bemidjiensis*; Glo, *Geobacter lovleyi*; Ppd, *Pelobacter propionicus*. The numbers refer to the gene that encodes for each cytochrome in the Keeg data base. The conserved residues in the proteins are boxed: heme attached (gray) and non-heme attached residues (black). The sequence identity (%) for each cytochrome in relation to PpcF is also indicated.



## 1.2. Methods



In order to understand the mechanisms underlying the extracellular electron transfer it is necessary to study their components. In the present work the focus was the triheme cytochromes from *G. metallireducens*. The detailed biochemical study of these proteins requires considerable amounts of material. Thus, it is not practical to isolate the proteins directly from *G. metallireducens*, because of the slow growth rates and required anaerobic conditions. In addition, due to the large amount of *c*-type cytochromes produced by *G. metallireducens* the purification of a target one is also more complex. Consequently, the first step of this work encompassed the cloning and expression of each protein in *E. coli*. The use of *E. coli* in heterologous expression holds up to the fact that there are a lot of expression vectors, absence of endogenous cytochromes expression during the fast aerobic growth, easy culture maintenance, and low cost. The second step of the protocol involved the purification of each cytochrome using cation exchange and molecular exclusion chromatography. For last, the proteins were preliminary characterized by mass spectrometry, UV-visible and NMR spectroscopy. An overview of the methodology used is described in Figure 6.

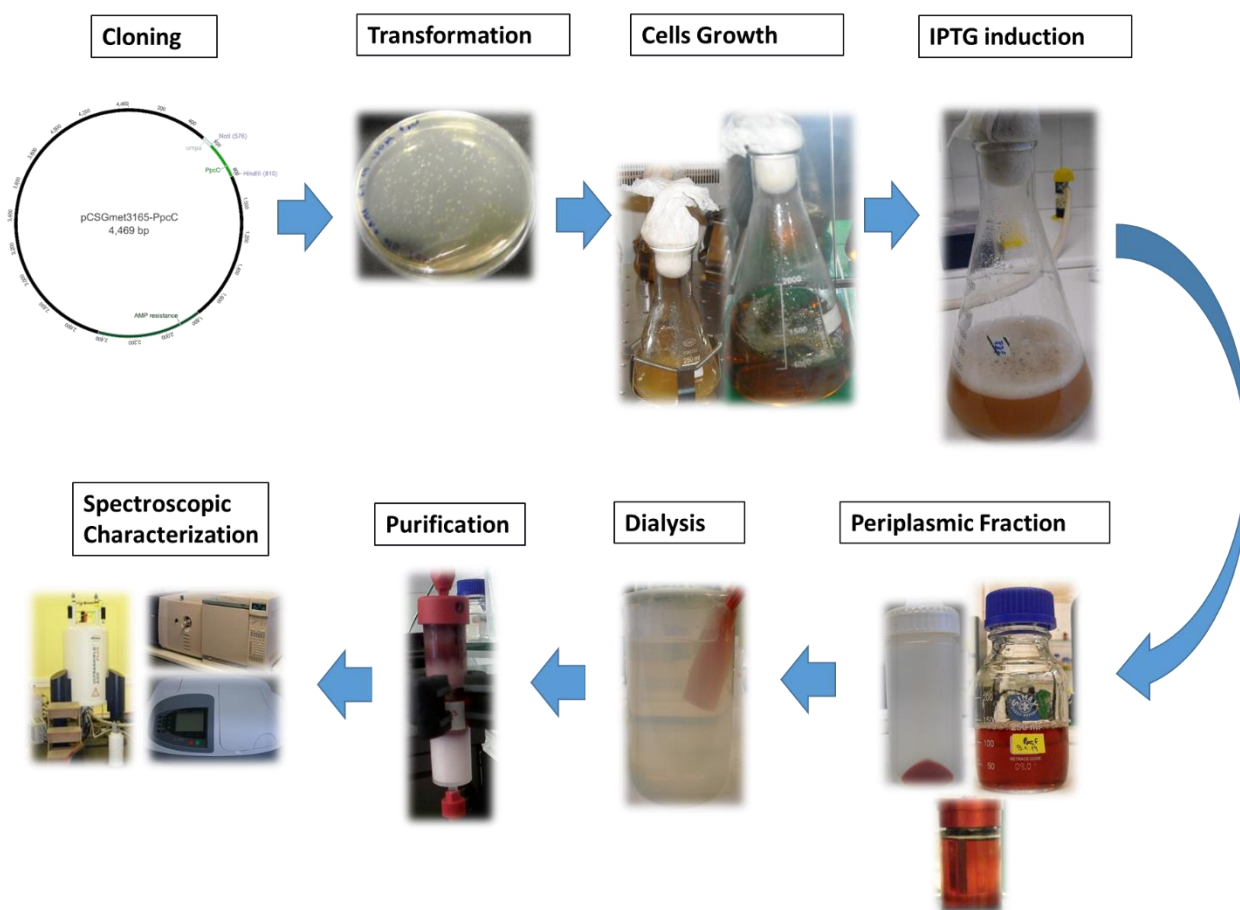


Figure 6: Overview of the methodology used to clone, produce, purify and characterize triheme cytochromes from *G. metallireducens*.



### 1.2.1. Cloning of cytochromes *c*<sub>7</sub> from *G. metallireducens*

Gene sequences for each triheme cytochrome from *G. metallireducens* studied in this work were obtained from Kyoto Encyclopedia of Genes and Genomes Web site ([http://www.genome.jp/kegg-bin/show\\_organism?org=gme](http://www.genome.jp/kegg-bin/show_organism?org=gme)). The accession numbers are listed in **Table 1**. Each triheme cytochrome was predicted to be located on the bacteria's periplasm. The prediction of the signal peptide cleavage site of each protein was calculated by bioinformatics tools, the Signal IP 4.1 server<sup>27</sup> and PSORT Prediction (<http://psort.hgc.jp/form.html>). This step allowed us to identify the soluble part of each protein for the cloning step (**Supplementary 4.1.A**).

**Table 1:** Access number in Kyoto Encyclopedia of Genes and Genomes Web site and signal peptide cleavage site calculated by two bioinformatics tools for the five periplasmic triheme cytochromes from *G. metallireducens*.

| Protein | Access number | Signal peptide Cleavage |       |
|---------|---------------|-------------------------|-------|
|         |               | Signal IP 4.1           | PSORT |
| PpcA    | Gmet_2902     | 20-21                   | 20    |
| PpcB    | Gmet_3166     | 20-21                   | 20    |
| PpcC    | Gmet_3165     | 23-24                   | 23    |
| PpcE    | Gmet_1846     | 20-21                   | 20    |
| PpcF    | Gmet_0335     | 22-23                   | 22    |

The primers for each gene sequence of the five triheme cytochromes and the expression vector that encodes for the PpcF protein were already available in the laboratory. Primers were purchased from Invitrogen, restriction enzymes and T4 DNA ligase from Fermentas.

The genes coding for PpcA, PpcB, PpcC and PpcE were amplified with primers containing restriction sites for the enzymes *HindIII* and *NotI* (**Table 2**) using Phusion High-Fidelity DNA polymerase (Finnzymes) (Program in **Supplementary 4.1.B, Table B-1**). Amplification products were purified using Wizard\_PCR Preps DNA Purification System (Promega). A 0.8% agarose gel electrophoresis was used to confirm the fragment size of each amplified PCR fragment. The digestion of the fragments was performed with the restriction enzymes *HindIII* (VWR) and *NotI* (Promega) at 37°C during ≈6 hours, and then 20 min at 65°C to inactivate the restriction enzymes.

The vector used for cloning was previously digested with the same restriction enzymes. This vector contains the lac promoter, the OmpA leader sequence and a resistance marker for ampicillin. Ligation of the fragment to the vector was carried out using a fragment:vector molar ratio of 5:1 and 3:1, during 1 hour at 22 °C, followed by a period of 20 minutes at 65°C. The

ligation product was transformed into *E. coli* DH5 $\alpha$  competent cells prepared by the calcium chloride method and plated for selection in LB medium supplemented with ampicillin (100  $\mu$ g/mL). The colonies were screened by colony PCR (Program in **Supplementary 4.1.B, Table B-2**) with pCK32 primers (pCK32\_fw: 5'-GGCTCGTATGTTGTGTGGAA-3' and pCK32\_rv: 5'-AAGGGAAGAAAGCGAAAGGA-3'). The amplification was performed using Taq DNA polymerase (VWR). After the confirmation of the fragment size by 0.8% agarose gel electrophoresis of the PCR product, the cells were grown in liquid LB medium supplemented with ampicillin for plasmid extraction and sequencing. All DNA quantifications were done in Nanodrop 1000 (Thermo Scientific).

**Table 2: Primers used to amplify the sequence of each protein.**

| Protein     | Primer                                    |   |
|-------------|---|---|
|             | Forward                                   | Reverse                                       |
| <b>PpcA</b> | CGGCCTTGCGGCCGCGCTGA<br>CGAGCTTACCTTCAAG  | CGCCGAAAGCTTCACCATTACTTCT<br>TGTGGCAATCGCCG   |
| <b>PpcB</b> | GCGGCGGCCGCGGCCGACACC<br>CTCAC            | CCGGCTGATTCGGCCGAAGCTTTTAC<br>TTCTTGTGGC      |
| <b>PpcC</b> | GAGCGGCGGCCGCGCCSTCGAGA<br>CCATTACCTTTC   | CGTCATAGACAAAGCTTCAACGAGTT<br>AGCCACCTCCGTGAC |
| <b>PpcE</b> | CGTACCCGTCGCGGCCGCTGC<br>GGATACCATGATATTC | CCGGCTAAGCTTGACATCAAGGGTG<br>CTACTTCCTGTGGTC  |
| <b>PpcF</b> | CACATGCGGCCGCGCCGACG<br>TATTTGAATTC       | GCCCCTACCGCAGGTTCAAGCTTTTA<br>CTTCTTGTGGCAG   |

The gene that encodes for the PpcB protein was not successfully cloned into the expression vector, using the previously described protocol. A different ligation protocol was tried: 25-50 ng of expression vector and three times more quantity of insert were mixed to a 100  $\mu$ l final volume. 1  $\mu$ l of glycogen, 1/10 of sodium acetate 3 M and three times the volume of absolute ethanol (300  $\mu$ l) were added to the previous mixture and were incubated during 1 h, at -70°C to precipitate the DNA. After that the mixture was centrifuged at 13,000 rpm, during 30 min, 4°C. The supernatant was rejected. Then we add 500 $\mu$ l of 70% ice ethanol to remove the salts. The tube was gently inverted to wash the pellet. After that the tube was centrifuged at 13,000 rpm during 15 min at 4°C. The supernatant was rejected. 10  $\mu$ l of DNA T4 ligase buffer, 9  $\mu$ l of milli-Q water autoclaved and 1  $\mu$ l of DNA T4 ligase were added to the pellet and placed overnight at 4°C.

### 1.2.2. Preparation of competent cell by the calcium chloride method

*Escherichia coli* cells, strain BL21, were streaked into Luria Bertani (LB) medium plate supplemented with 34 µg/mL chloramphenicol (CLO) from NZYtech and incubated at 37°C, overnight. A single colony was selected from the plate and inoculated in 5 mL of LB medium supplemented with 34 µg/mL of CLO. The inoculums were grown at 37°C overnight (200 rpm) and then 500 µL of that culture was transferred into 50 mL LB medium supplemented with the same antibiotic. Cultures were grown at 37 °C, 200 rpm, until reached an OD<sub>600</sub> between 0.4 and 0.6 (approximately during 3 hours).

Cells were harvested by centrifugation at 2,500 *xg* during 15 min at 4°C. The pellet was gently resuspended in 10 mL of ice cold 0.1M CaCl<sub>2</sub> and incubated on ice during 1 hour. The cells were then centrifuged at 2,500 *xg*, 10 min, 4°C. The supernatant was removed and the cell pellet was resuspended in 2 mL of pre-cooled 0.1 M CaCl<sub>2</sub> solution and 0.5 mL of pre-cooled 80% glycerol.

### 1.2.3. Bacterial growth

*Escherichia coli* is the most common expression host in the heterologous expression of multiheme proteins. The gene cluster, *ccmABCDEFGHIH* is responsible for maturation of *c*-type cytochromes under anaerobic conditions in *E. coli*. To preserve this characteristic in aerobic conditions the gene cluster was cloned to vector pACYC184<sup>28</sup>, renamed pEC86<sup>29</sup>. The co-expression of pEC86 with a second plasmid pCK32, a pUC derivate, which harbors the gene sequence that encodes for each triheme cytochrome, OmpA leader sequence (drive the new polypeptide to periplasm), a resistance marker for chloramphenicol and *lac* promoter allows the heterologous expression of *c*-type cytochromes in *E. coli* under aerobic conditions<sup>30</sup>.

In this system, the *lac* promoter on pCK32 plasmid is induced by addition of isopropyl-β-D-1-thiogalactopyranoside (IPTG) from NZYtech. This inductor is a non-metabolizable substrate analog of lactose, which induces the expression of *lac* operon in *E. coli*. The mechanism of action involves the IPTG ligation to the *lac* repressor, causing the alteration of its conformation. The inactivation prevents the repression, thus allowing the transcription of genes contained in this operon, it means that after the IPTG induction, the gene harboring the *c*-type cytochrome is expressed<sup>30</sup>.

*E. coli* strain BL21 containing the plasmid pEC86<sup>29</sup> (prepared in **Section 1.2.2**) was co-transformed with the plasmid pCK32, the expression vector harboring the gene sequence encoding for each triheme cytochrome. Transformed *E. coli* cells were grown in 2x yeast extract-tryptone (2xYT) supplemented with 34 µg/ml chloramphenicol (CLO) and 100 µg/ml ampicillin (AMP), both from NZYtech. Colonies were selected and aerobically grown until an OD<sub>600</sub> between 1.8 and 2 at 30°C, 200 rpm and overnight. 0.1% of this culture was transferred to 1L of 2xYT medium, also supplemented with 34µg/mL CLO and 100µg/mL AMP and grown for approximately 10 hours at 30°C and 180 rpm. When the cultures reached an OD<sub>600</sub> > 1.5,

the protein expression was induced with 10  $\mu\text{M}$  of IPTG<sup>24</sup>. After overnight incubation at 30°C and 160 rpm, cells were harvested by centrifugation at 4000 xg, 20 min and 4 °C. The cell pellet was gently resuspended in 30 mL of lysis buffer (20% sucrose (Panreac), 100 mM Tris-HCl (NZYtech) pH 8.0 and 0.5 mM EDTA (Sigma) containing 0.5 mg/mL of lysozyme (Merck)), per liter of initial cell culture. Then the suspension was incubated at room temperature during 15 min and after 15 min on ice with gently shaking. Finally, the cells were centrifuged at 14,700xg, 20 min at 4 °C. The supernatant constituted the periplasmic fraction, which was ultracentrifuged at 44,000xg during 1h and 30 min at 4 °C.

#### 1.2.4. Expression tests: PpcC and PpcE

The yield of PpcC and PpcE obtained was too low, so it was necessary to test different conditions. The protocol used for bacterial growth was the same described in **1.2.3. Section** with the exception that four different IPTG (NZYtech) concentrations: 50  $\mu\text{M}$ , 100  $\mu\text{M}$ , 200  $\mu\text{M}$  and 300  $\mu\text{M}$  were used.

#### 1.2.5. Protein purification

The purification of the proteins was performed using two chromatographic methods: cation exchange and molecular exclusion. The isoelectric point for each protein was estimated using ExPASy Mw PI tools<sup>31</sup>.

Periplasmic fraction was first dialysed against 10 mM Tris-HCl pH 8 (MWCO 3500). After that, was injected in a cation exchange column 2x5 ml HiTrap SP HP (GE Healthcare) equilibrated with 10 mM Tris-HCl pH 8. The proteins were eluted with a gradient from 0 to 300 mM NaCl. For molecular exclusion chromatography, the red colored fractions obtained from cation exchange step were pooled together and concentrated to 1 mL and then injected in a Superdex 75 molecular exclusion column (GE Healthcare) equilibrated with 100 mM sodium phosphate buffer, pH 8. Protein was eluted at flow rate 1mL/min. Both chromatography steps were performed in an ÄKTA Prime Plus FPLC System (GE, Amersham). The presence of the cytochrome was confirmed by sodium dodecyl sulfate polyacrylamide gel electrophoresis (SDS-PAGE) stained with Coomassie Blue or by TMBZ/H<sub>2</sub>O<sub>2</sub> to detect hemes (see **Supplementary, Table L-1** and **Table L-2**). The protein concentration was determined by UV-visible spectroscopy using the specific absorption coefficient calculated for the  $\alpha$ -band of the PpcA from *G. sulfurreducens*<sup>33</sup>. The spectra were acquired using the spectrophotometer (Ultrospec 2100pro Amersham Biosciences).

### 1.2.6 NMR experiments

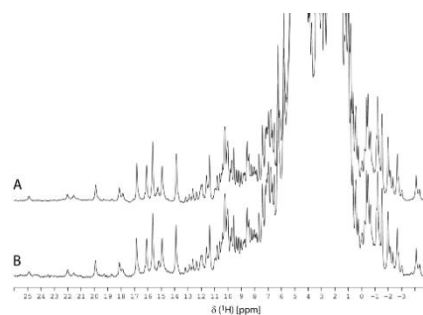
All of the NMR experiments were acquired in a Bruker Avance III 600 MHz spectrometer equipped with a triple-resonance cryoprobe (TCI) available at Faculdade de Ciências e Tecnologia, Universidade Nova de Lisboa.  $^1\text{H}$  chemical shifts were calibrated using the water signal as internal reference:

$$\delta_{\text{H}_2\text{O}} = 5.11 - 0.012T \text{ (}^\circ\text{C)}^{34} \quad \text{Equation 1}$$

Spectra were processed using TopSpin (Bruker BioSpin, Karlsruhe, Germany). 1D- $^1\text{H}$  NMR spectra were recorded before and after protein lyophilization to check proteins' integrity. The pH sample was measured with a glass micro electrode (Crison). Oxidized samples of PpcA and PpcF of *G. metallireducens* (70  $\mu\text{M}$ ) were prepared in 80 mM sodium phosphate buffer with NaCl (final ionic strength of 250 mM) in 92%  $\text{H}_2\text{O}/8\%$   $^2\text{H}_2\text{O}$ .



## 1.3. Results and discussion



### 1.3.1. Cloning of $c_7$ cytochromes from *G. metallireducens* $c_7$

The gene encoding for each triheme cytochrome from *G. metallireducens* was firstly cloned in the expression vector pCK32 and the resulting vectors were called pCSGMET2902, pCSGMET3165, pCSGMET1846 and pCSGMET0335 that encode for PpcA, PpcC, PpcE and PpcF, respectively. Only the results obtained for PpcA are presented in this section, since the cloning protocol was similar for each protein. The results obtained for the remaining proteins are given in the supplementary section.

The correct size of the PCR fragments was evaluated by gel electrophoresis, as described in Figure 7 for PpcA.

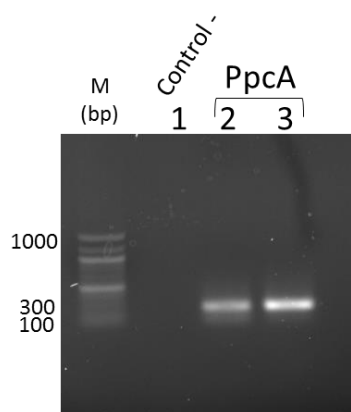


**Figure 7: Gel electrophoresis 0.8% to evaluate the quality of PCR fragments.** From left to the right, Gene ruler 100 bp DNA ladder (M), negative control (without DNA) and two PCR fragment amplified. PpcA (336 bp).

The analysis of **Figure 7** shows that there is no amplification in the negative control. On the other hand, the size of PpcA amplified fragment corresponds to the expected size (336 bp). A similar result was obtained for PpcC (**Supplementary Figure C-1**). In contrast, for PpcB and PpcE the negative controls appear to have a contamination (**Supplementary Figures C-1**). However, the amplified fragments appeared the correct size (336 bp) and therefore the cloning protocol was also carried out for PpcB and PpcE.

After ligation, a screening by colony PCR was performed and the fragments obtained were analyzed by gel electrophoresis (**Figure 8**).

The expected size for PpcA colonies fragment obtained from the amplification of the plasmid with the pCK32 primers is 571 bp. Therefore, the colonies numbered #1, #2, #8 and #12 were selected for sequencing. The sequencing results indicated that only colony #2 presented the correct sequence (**Supplementary Figure D-1**).

The gel electrophoresis obtained with the fragments resulting from the PCR of colonies transformed with plasmid containing the genes coding for the other triheme cytochromes are indicated in the **Supplementary Figure C-2 and Figure C-3**. In the case of PpcC and PpcE the colonies that appeared to have the correct size (579, 580 respectively) were selected for sequencing. The results obtained showed that all the selected colonies had the correct sequence (**Supplementary Figure D-1**). In contrast, no bands were observed in the gel electrophoresis obtained from PCR of colonies of PpcB (**Supplementary Figure C-2**),. In this



case, a different protocol was performed but unfortunately it was also not possible to obtain the plasmid coding for PpcB. The results obtained for PpcB using this alternative protocol are described in **Supplementary Figure C-4**.

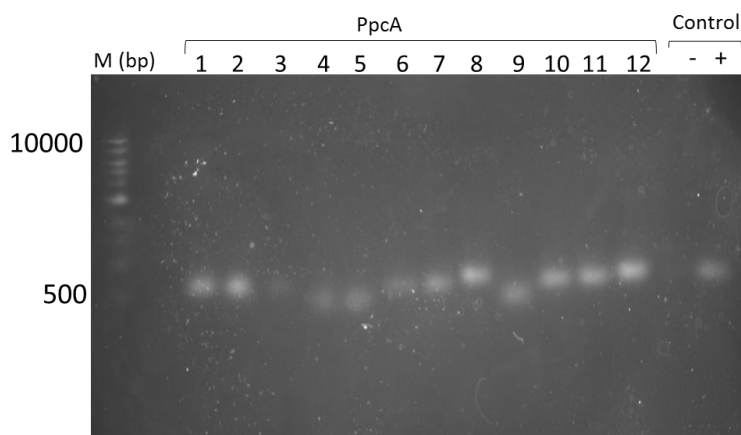


**Figure 8: Gel electrophoresis 0.8% resulting from PCR of colonies of PpcA.** From left to the right, Gene ruler 1 Kb DNA ladder, bank space, PCR fragment amplified corresponding to PpcA (1,2,3,...,12), negative and positive controls.

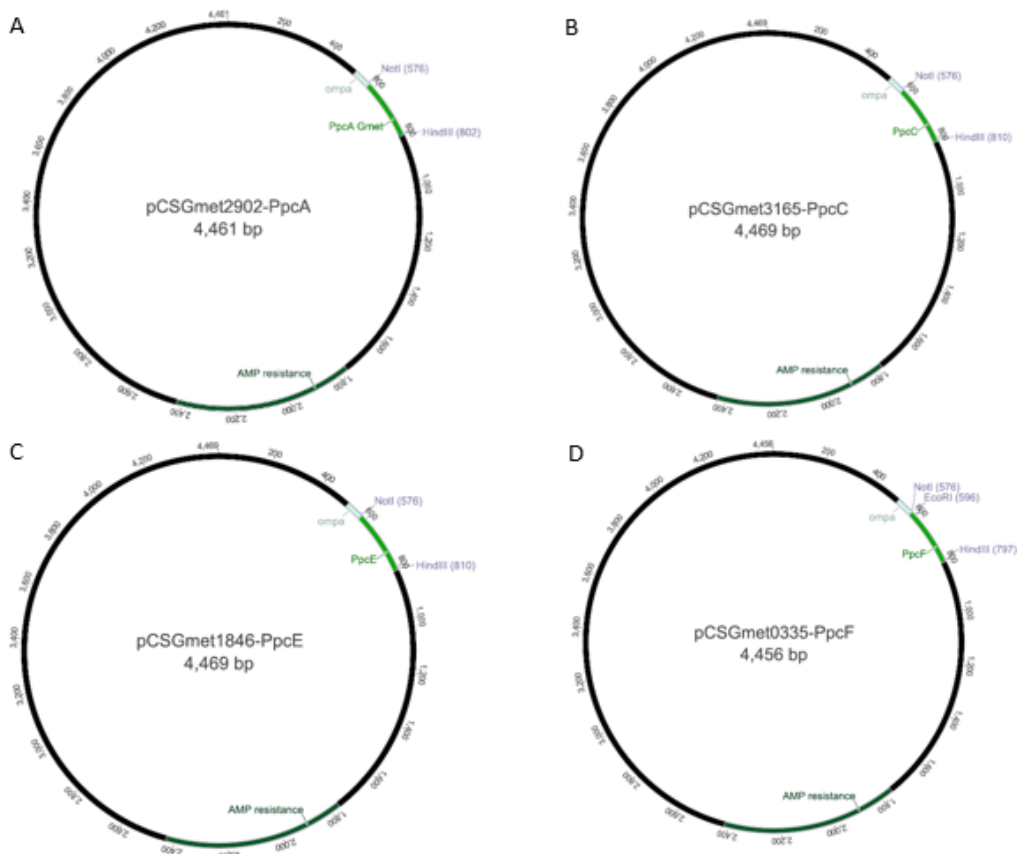


**Figure 9: A - Plasmid pCSGmet2902-PpcA resulting from the cloning of PpcA sequence. B - Plasmid pCSGmet3165-PpcC resulting from the cloning of PpcC sequence. C - Plasmid pCSGmet3166-PpcE resulting from the cloning of PpcC sequence. D - Plasmid pCSGmet0335-PpcF resulting from the cloning of PpcC sequence.**

To sum up, it was possible to clone the genes coding for PpcA, PpcC, PpcE and PpcF cytochromes in the pCK32 plasmid. The obtained plasmids were designated pCSGmet2902-PpcA, pCSGmet3165-PpcC, pCSGmet1846-PpcE and pCSGmet0335-PpcF. (Figure 9). The gene coding for PpcF was already cloned in the laboratory (pCSGmet3166-PpcF).

### 1.3.2 Heterologous expression of $c_7$ cytochromes from *G. metallireducens*

*Escherichia coli* was used as host, because it presents an efficient expression system to produce multiheme *c*-type cytochromes. This system has already been described and successfully applied to the expression of multiheme cytochromes containing up to 12 heme groups<sup>19,30</sup>. During the bacterial growth, and particularly after cell harvesting, the reddish pellets are indicative of a successful expression of the target cytochrome. This was observed for cells expressing PpcA and PpcF but not for PpcC and PpcE (Figure 10).

In the case of the two latter cytochromes the lower yields (Table 3) can be attributed to the amount of IPTG used. As mentioned in the Methods section, 10  $\mu$ M IPTG was used by analogy to that used to express triheme cytochromes from *G. sulfurreducens*. In order to confirm this hypothesis expression tests were carried out for PpcC and PpcE cytochromes. Analysis of the protein content of the periplasmic fractions by SDS-PAGE indicates that 100  $\mu$ M IPTG concentration is the more promising concentration to express PpcE (Figure 11) and explain the low yields obtained with 10  $\mu$ M IPTG. In the SDS-PAGE stained by TMBZ/H<sub>2</sub>O<sub>2</sub> a band that might correspond to PpcE is observed for all IPTG concentrations used.

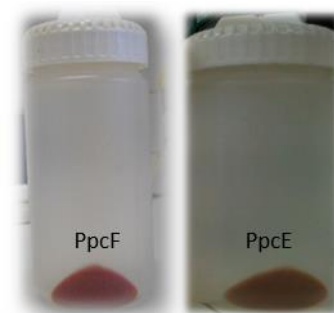


Figure 10: Pellets from periplasmic fraction of PpcF (red) and PpcE (brown-reddish).

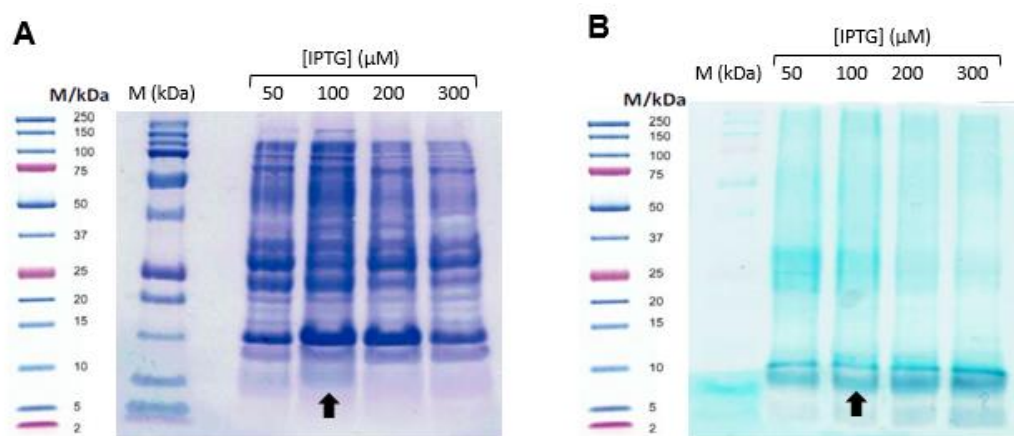
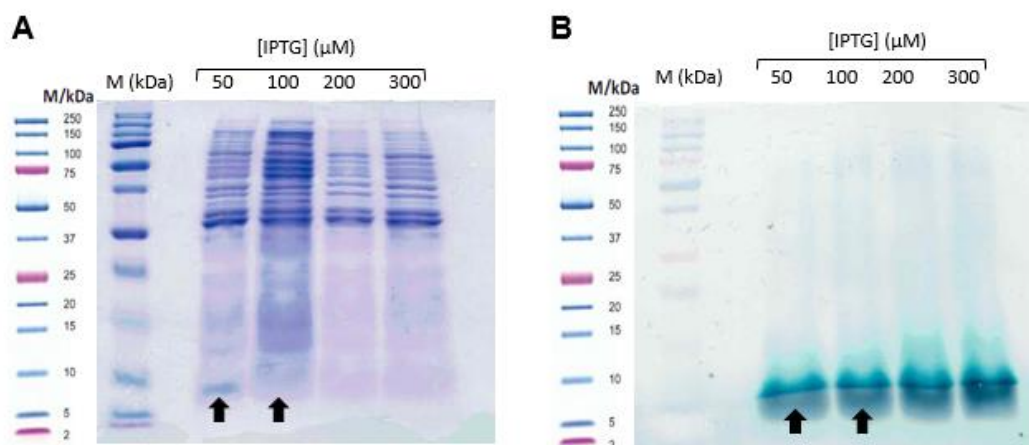


Figure 11: SDS-PAGE electrophoresis gel stained with Coomassie blue (A) and TMBZ/H<sub>2</sub>O<sub>2</sub> (B) for the periplasmic fractions of PpcE obtained from cell cultures induced with different concentrations of IPTG. From the left to the right: marker Precision plus protein™ Dual Xtra Standards (M), periplasmic fraction obtained from cell cultures induced with 50  $\mu$ M, 100  $\mu$ M, 200  $\mu$ M, 300  $\mu$ M IPTG. The best concentration is indicated with a black arrow.

On the other hand, the expression tests for cytochrome PpcC were not very conclusive (Figure 12). In the heme staining SDS-PAGE it is visible one band that corresponds to the PpcC at ~10 kDa in all IPTG concentrations used. Regardless, the expression yields were very low to allow for characterization of PpcC (see below). Therefore, for this cytochrome other expression vectors and conditions (such as temperature) need to be tested in order to optimize the protein expression.



**Figure 12: SDS-PAGE electrophoresis gel stained with Coomassie blue (A) and TMBZ/H<sub>2</sub>O<sub>2</sub> (B) for the periplasmic fractions of PpcC obtained from cell cultures induced with different concentrations of IPTG.** From the left to the right: marker Precision plus protein<sup>tm</sup> Dual Xtra Standards (M), periplasmic fraction obtained from cell cultures induced with 50 μM, 100 μM, 200 μM, 300 μM IPTG. The best concentration is indicated with a black arrow.

### 1.3.3. Protein purification and expression yields

As described in the Methods section, the purification of the four triheme cytochromes (PpcA, PpcC, PpcE and PpcF) followed an identical methodology. After the expression, the proteins were purified by cation exchange followed by molecular exclusion chromatography. The progress of the purification was monitored by SDS-PAGE electrophoresis.

Due to the high isoelectric point of these cytochromes (**Supplementary Table H-1**) the proteins strongly bind to the cation exchange column at pH 8. The bound proteins were then eluted with a NaCl gradient ranging from 0 to 300 mM. Each protein of interest was eluted at different percentage as is represented in (**Supplementary Table H-1**).

The elution profile of the cationic exchange column showed two intense peaks that are eluted at 65 % and 74 % of NaCl gradient (**Figure 13**).

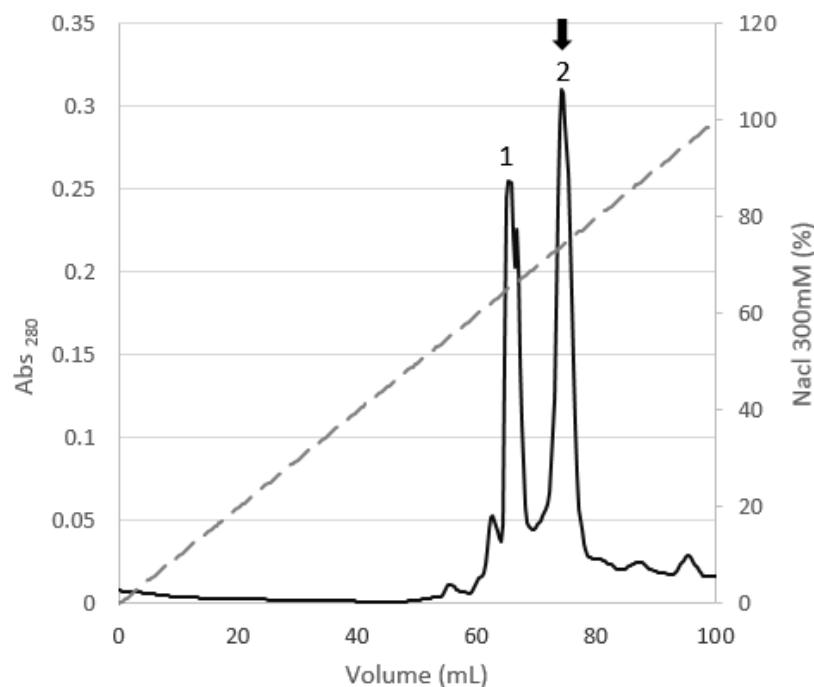


**Figure 13: Elution profile for the cation exchange column chromatography equilibrated with 10 mM Tris-HCl, pH 8 (flow rate of 1 ml/min) for PpcA.** Primary and second y-axis, represent the variation of absorbance at 280 nm (dark solid line) and the NaCl gradient profile (grey dashed line), respectively. PpcA correspond to the second peak (black arrow).

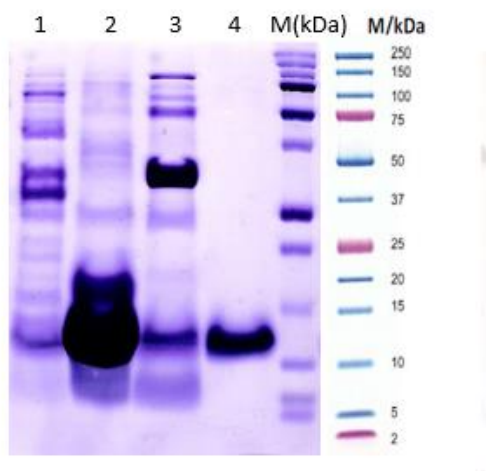


**Figure 14: SDS-PAGE electrophoresis gel stained with Coomassie blue for the main peaks obtained in the chromatographic purification steps of PpcA.** From the left to the right: 1- periplasmic fraction; 2- cation exchange column chromatography band #2; 3- cation exchange column chromatography band #1, 4- molecular exclusion column chromatography band and marker precision plus protein™ Dual Xtra Standards (M).

The fractions correspondent to these two peaks were combined separately and analyzed by SDS-PAGE electrophoresis (**Figure 14**).

The fraction corresponded to peak 2 in the cation exchange chromatography was further purified by molecular exclusion chromatography (**Figure 15**) and the protein of interest was eluted at different volumes with 100 mM sodium phosphate buffer, pH 8 (**Supplementary Table H-2**). After this purification step, only one band was observed in the SDS-PAGE electrophoresis (**Figure 14**) and corresponds to a MW of approximately 10 kDa.

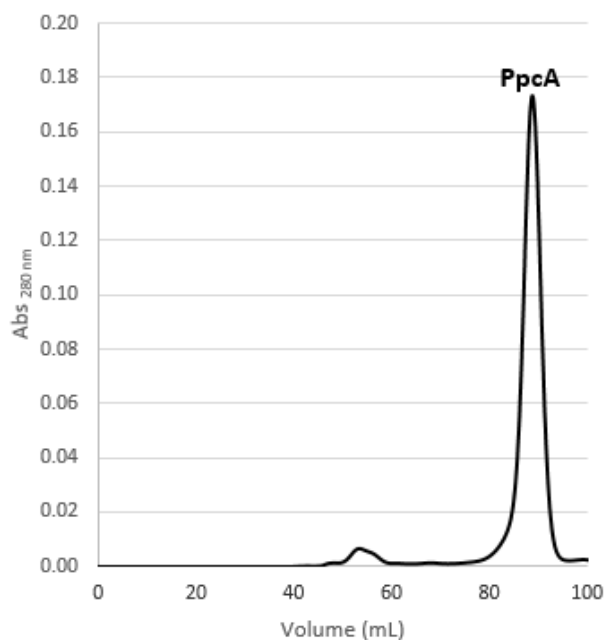


**Figure 15: Elution profile for the molecular exclusion column chromatography equilibrated with 100 mM sodium phosphate buffer, pH 8 for PpcA. PpcA eluted at 85 ml.**

Although PpcF was already cloned in the laboratory, no attempts had been made to express and purify it. The expression was successfully achieved in the present work but there were some problems during the purification of this protein. In the cationic exchange

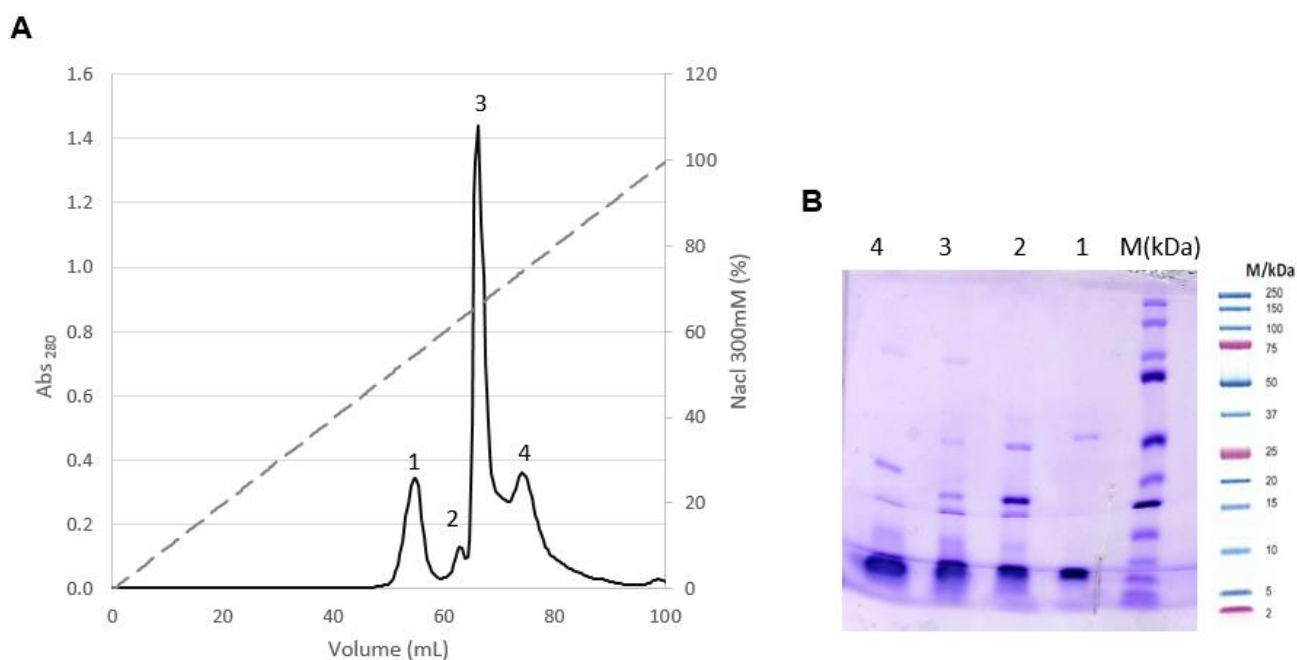


**Figure 16: A- Elution profile for the cation exchange column chromatography equilibrated with 10 mM Tris-HCl, pH 8 for PpcF (flow rate of 1 ml/min). Primary and second y-axis , represent the variation of absorbance at 280 nm (dark solid line) and the NaCl gradient profile (grey dashed line), respectively. PpcF eluted 55%, 65%, 70% and 75%. B- SDS-PAGE electrophoresis gel stained with Coomassie blue from the collected fractions during the cation exchange column chromatography. Each number in the SDS-PAGE corresponds to a band in the chromatogram. Lane M corresponds to the marker Precision plus protein<sup>™</sup> Dual Xtra Standards.**

chromatography, four bands were obtained (Supplementary Figure 18A). The analysis of the SDS-PAGE gel indicates that the target protein is present in each fraction.

Each fraction obtained in the cation exchange chromatography was purified in separate by molecular exclusion chromatography. The elution profiles obtained are indicated in (Figure 17).

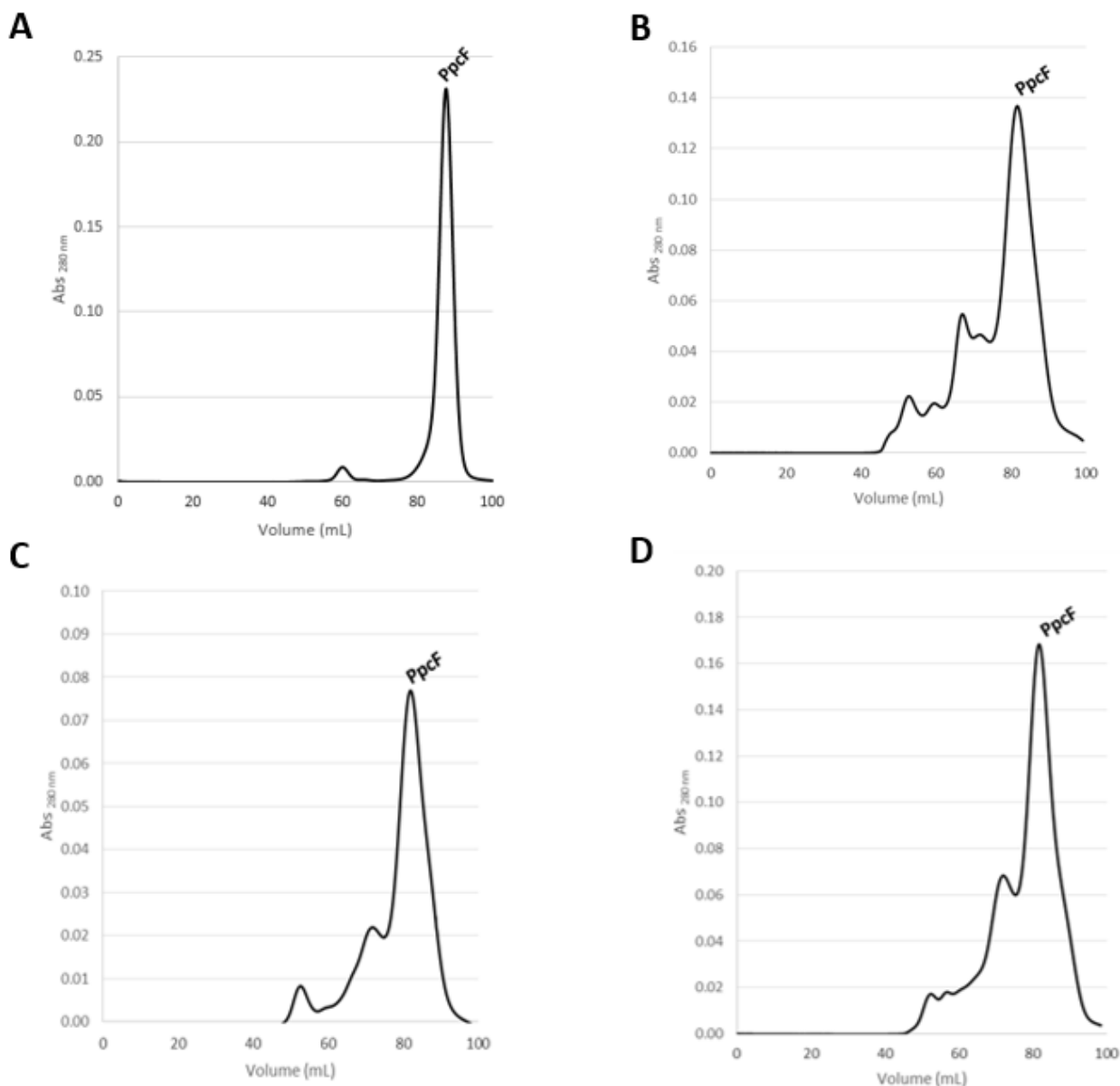


**Figure 17: Elution profile obtained in molecular exclusion column chromatography for each band (1-4) obtained in the cationic exchange chromatography step for PpcF.** (A) band 1; (B) band 2; (C) band 3, (D) band 4.

The fractions correspondent to the more intense bands obtained in the molecular exclusion chromatography were analyzed by SDS-PAGE (Figure 18). The results showed a single band at the expected molecular weight for PpcF.

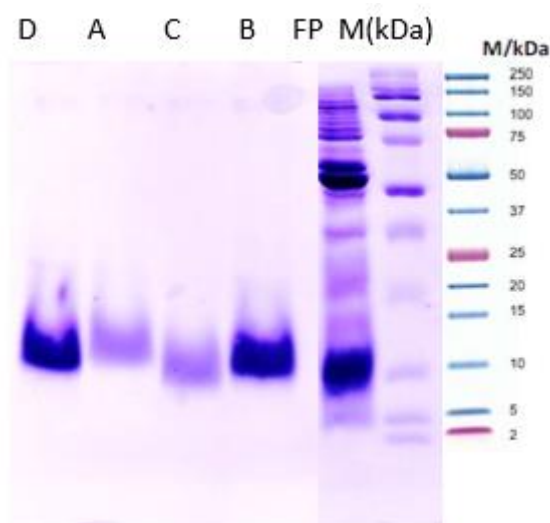


**Figure 18: SDS-PAGE electrophoresis gel stained with Coomassie Blue correspondent to the fractions of the more intense band obtained in the molecular exclusion chromatography of PpcF purification procedure. A-D correspond to panels indicated in Figure 17.**

Although the purification of PpcF was successfully achieved at pH 8, slightly modifications to the purification protocol were investigated in order to optimize the ionic exchange chromatography step. In fact, purification of PpcF was also carried out at pH 7.5 and 8.5 (see **Supplementary Figures E-1 and E-2**). However no major improvements were obtained from these alterations.

The elution profiles obtained for the purification of cytochromes PpcC and PpcE are indicated in supplementary material (**Supplementary Figures F-1 and F-2** for PpcC and **Figures G-1 and G-2** for PpcE). The SDS-PAGE electrophoresis gels stained with Coomassie blue and TMBZ/H<sub>2</sub>O<sub>2</sub> (**Supplementary Figures F-3 and G-3** for PpcC and PpcE, respectively) indicates that after the molecular exclusion chromatography step both proteins are not entirely pure. This indicates that the purification protocol for PpcC and PpcE requires further optimization.

Protein yields were quantified by visible spectroscopy using the PpcA from *G. sulfurreducens* extinction absorption coefficient of the  $\alpha$  band characteristic of the protein reduced form ( $\epsilon_{552} = 97.5 \text{ mM}^{-1} \text{ cm}^{-1}$ )<sup>33</sup>. The yields obtained are indicated in **Table 3**.

**Table 3: Expression yields for triheme cytochromes from *G. metallireducens*.**

| Protein | Expression yield (mg/L cell culture)* |
|---------|---------------------------------------|
| PpcA    | 1.95                                  |
| PpcB    | -                                     |
| PpcC    | 0.14                                  |
| PpcE    | 0.02                                  |
| PpcF    | 1.16                                  |

### 1.3.4. Protein characterization

Due to the low expression yields of PpcC and PpcE only PpcA and PpcF molecular mass was confirmed by MALDI-TOF-MS. In the case of PpcA, the more intense peak in the mass spectrum corresponds to a molecular mass of 9691.48 Da  $\pm$  0.05% (**Supplementary Figure I-1**). The value obtained is slightly above the error compared with the expected value for the mature PpcA (9682.58 Da; see **Supplementary Table H-1**). In the case of PpcF, the value obtained from the mass spectrum corresponds to a molecular mass of 9739.80 Da  $\pm$  0.05% (**Supplementary Figure I-2**), which is in agreement with the predicted value for mature PpcF (9735.71 Da; see **Supplementary Table H-1**). For both measurements the equipment was externally calibrated with a horse cytochrome sample, which might explain the deviations observed.

The optical absorption spectrum of PpcA has an intense peak (Soret) at 412 nm. Upon reduction the protein shows the Soret,  $\beta$  and  $\alpha$  bands at 419 nm, 523 nm and 552 nm, respectively (**Figure 19**).

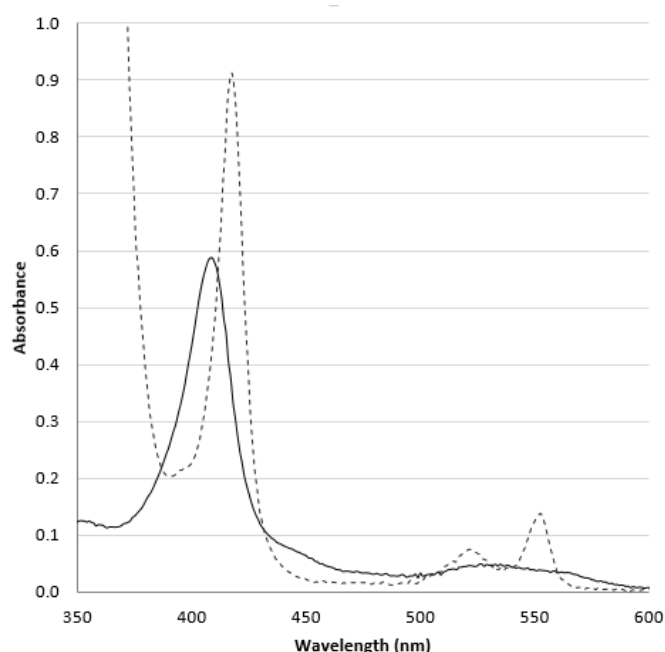


**Figure 19: Visible absorption spectra of PpcA in the oxidized (solid line) and reduced (dashed line) forms.**

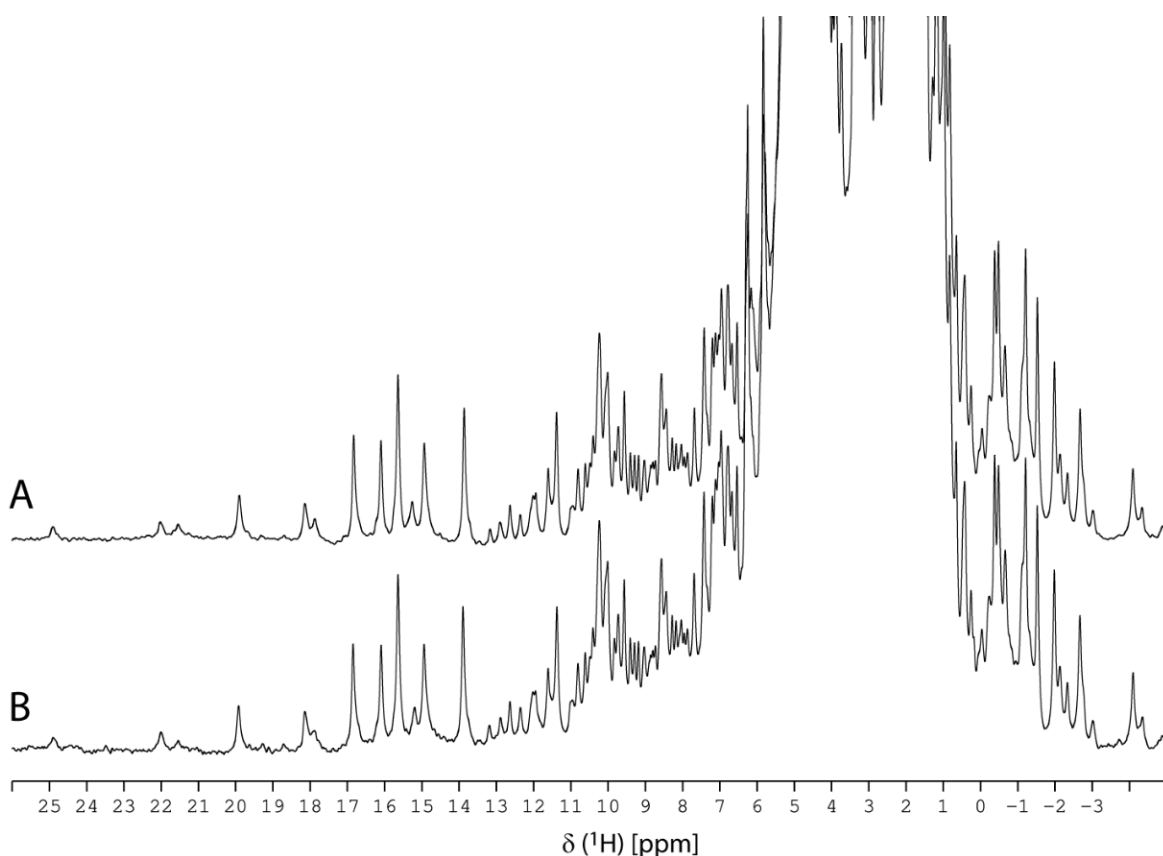
Similarly, for the other three proteins (PpcC, PpcE and PpcF) the optical absorption spectra in the oxidized and reduced form are typical of low-spin hexacoordinated *c*-type cytochrome (see **Supplementary J**). The optical absorption maxima values for each cytochrome in oxidized and reduced forms are summarized in the **Table 4**.



**Table 4: Summary of the optical absorption maxima in oxidized and reduced spectra for each triheme cytochrome from *G. metallireducens*.**

| Optical absorption(nm) |                | PpcA | PpcC | PpcE | PpcF |
|------------------------|----------------|------|------|------|------|
| Oxidized               | Soret          | 412  | 410  | 406  | 410  |
| Reduced                | Soret          | 419  | 418  | 419  | 421  |
|                        | $\beta$ -band  | 523  | 521  | 519  | 523  |
|                        | $\alpha$ -band | 552  | 553  | 550  | 552  |

In addition to the optical spectroscopy and mass spectrometry characterization, we also probed the features of PpcA and PpcF in 1D  $^1\text{H}$  NMR spectra. For both proteins spectra were acquired before and after lyophilization to evaluate their integrity. The comparison of the spectra showed that the spectra are similar (**Figure 20, Supplementary Figure K-1**).

**Figure 20: 1D- $^1\text{H}$  NMR spectra of PpcA (70  $\mu\text{M}$ ) obtained at 25  $^{\circ}\text{C}$  before (A) and after (B) lyophilization.**

The 1D  $^1\text{H}$  NMR spectra of the reduced and oxidized state for PpcA and PpcF are indicated in **Figure 21** and **Supplementary Figure K-2**, respectively. The NMR spectra corroborate the data obtained in the visible spectra. In fact, the spectra are typical of low-spin  $c$ -

type cytochromes showing signals in the reduced and oxidized states below 12 and 20 ppm, respectively.

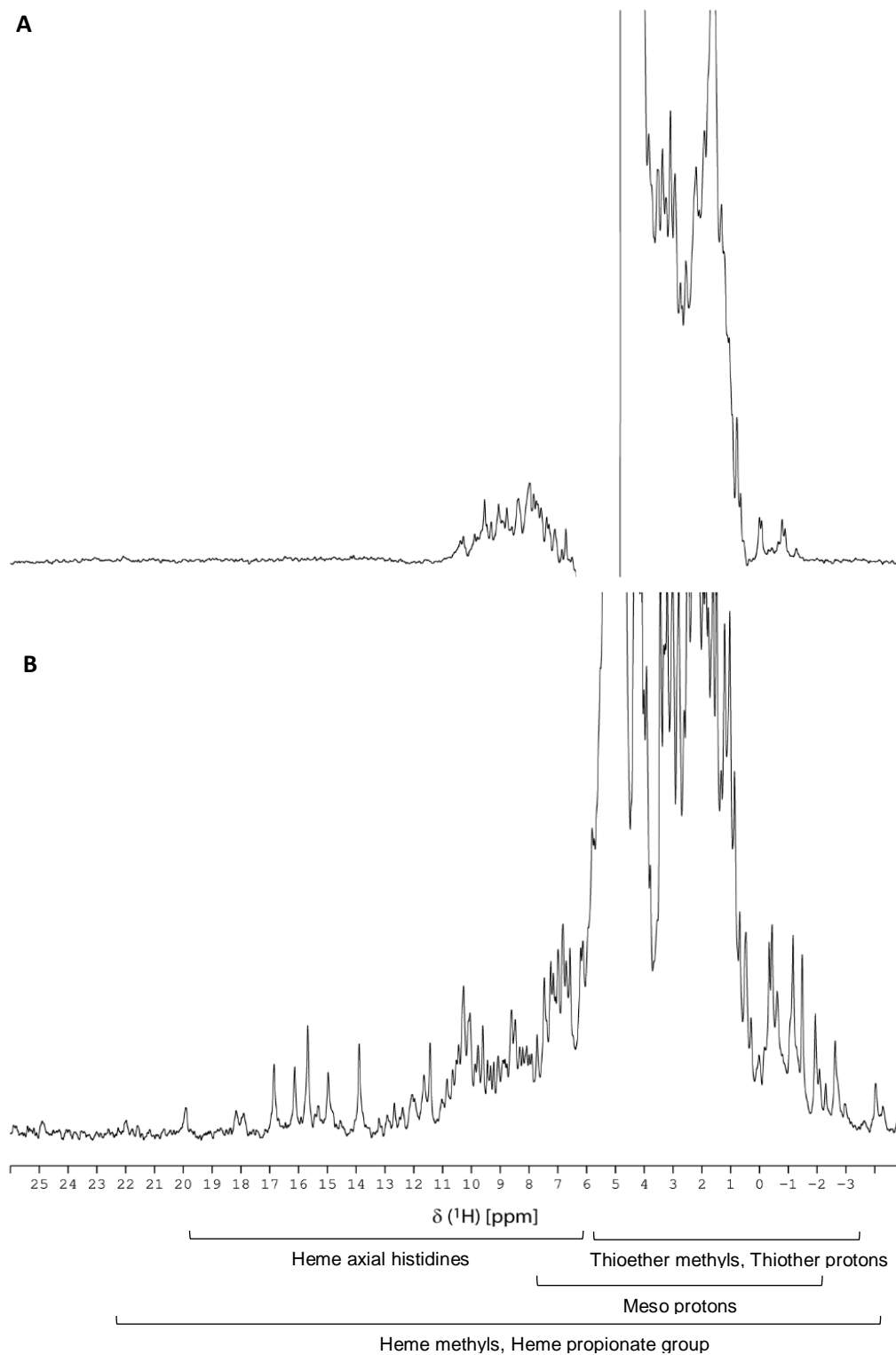


**Figure 21:** 1D- $^1\text{H}$  NMR spectra of the reduced (A) and oxidized (B) triheme cytochrome PpcA (70  $\mu\text{M}$ ) obtained at 25  $^\circ\text{C}$ , pH 8. The typical regions of the heme substituents in the oxidized spectrum are indicated.

#### 1.4. Future Work

This work constitutes the first step towards the elucidation of the role of periplasmic triheme cytochromes in *G. metallireducens* and the concomitant optimization of the biotechnological applications driven by these bacteria. In order to achieve this goal it is first necessary to clone, express and purify each protein. With exception of PpcB all the proteins were successfully cloned and expressed. However the expression yields of cytochromes PpcC and PpcE requires further optimization. Therefore, efforts to further optimize the expression of these cytochromes should be one of the goals to pursuit in the near future. The present work also sets the stage for a detailed characterization of cytochromes PpcA and PpcF. This should include the determination of the detailed thermodynamic and kinetics properties of these cytochromes, as well as their structures. In addition to this, the identification of the NH signals of each protein is crucial to identify their putative redox partners.



## 2. Chapter II

### Pcch, a new class of monohemic cytochrome

The results shown in this chapter have been published in the paper Dantas JM, Campelo LM, Duke NEC, Salgueiro CA, Pokkuluri PR (2015) "The structure of Pcch from *Geobacter sulfurreducens* – a novel low reduction potential monoheme cytochrome essential for accepting electrons from an electrode", FEBS Journal, 282, 2215-2231

My contribution to this work was the production and analysis of the dendograms presented in the section "Pcch, a new class of monohemic cytochrome".



## 2.1. Introduction



*Geobacter* spp. demonstrated an amazing respiratory versatility that confers these bacteria a highly relevant role in the biogeochemistry of several anaerobic environments. These capabilities show a huge potential for *Geobacter* based applications in bioenergy production and bioremediation<sup>35</sup>. Since these bacteria can use insoluble electron donors and acceptors besides the common soluble compounds. The use of compounds that cannot freely diffuse into and from cells requires that microorganisms be capable of extracellular electron exchange. This principle represented the *Geobacter*-based bioenergy strategies, like microbial fuel cells and microbial electrosynthesis.

Microbe-electrode exchange is also required for microbial electrosynthesis in which microorganisms use electrons supplied by electrodes for the reduction of carbon dioxide to multicarbon fuels or other organic commodity chemicals. The establishment of an efficient microbe–electrode exchange by *Geobacter* spp. and other electrogenic bacteria, such as *Shewanella* spp., requires the participation of electron transfer proteins to link intracellular oxidative reactions to extracellular reductions beyond the outer membrane and vice-versa. Ross et al.<sup>36</sup> showed that the Mtr respiratory pathway, which catalyzes electron flow from cytoplasmic oxidative reactions to electrodes in *Shewanella oneidensis* strain MR-1, is also used for the electrode-dependent fumarate reduction

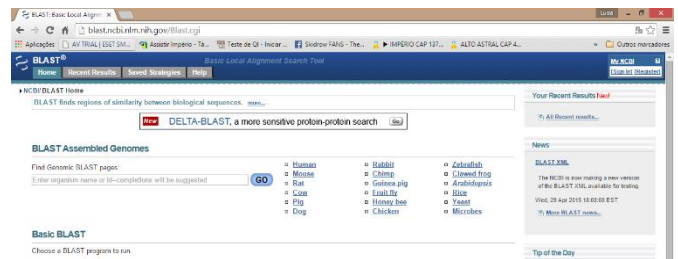
Studies analyzing the gene transcript abundance in current-consuming *versus* current-producing of *G. sulfurreducens* biofilms reveal that electrode-dependent fumarate reduction was independent of major outer membrane cytochromes required for extracellular electron exchange. The fumarate reduction was dependent from the monoheme c-type cytochrome designated PcCH<sup>37</sup>. Deletion of gene *pcch* completely inhibited electron transfer from electrodes but had no influence on electron transfer to electrodes, which suggest different routes for electron transfer into and out of the cell in *G. sulfurreducens*.

PcCH is characterized a basic protein with a polypeptide chain length of 129 amino acids that contains a typical heme-binding CXXCH sequence close to the N-terminus. The structure of PcCH, taken together with the sequence comparisons, suggests that this cytochrome forms the first characterized representative of a new subclass of monoheme cytochromes. To the best of our knowledge, PcCH is the first c-type monoheme cytochrome showing a negative reduction potential value within the physiological pH range of growth for *G. sulfurreducens*. This feature permits the protein to be redox active at the typically negative working potential ranges encountered by this bacterium.

The main purpose of the manuscript that includes the bioinformatics contribution described in this chapter was the report of the cytochrome PcCH X-ray crystal structure. Structural information for this cytochrome is important in interpreting the physicochemical data, such as thermodynamic and kinetic properties, which in turn is essential for determining the electron transport events and molecular mechanisms involved in *G. sulfurreducens* current-consuming biofilms.

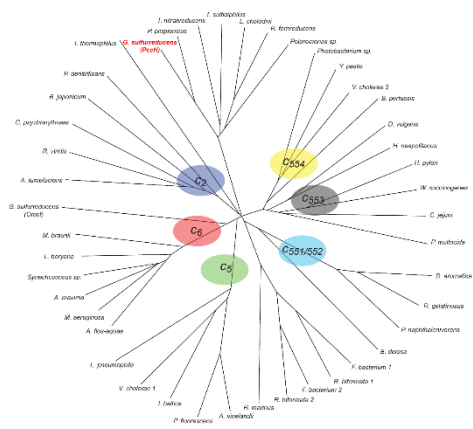


## 2.2. Methods



Amino acid sequence comparisons were performed using BLAST at the NCBI <sup>38</sup>. Multiple sequence alignments and dendograms were produced using CLUSTAL X2 <sup>39</sup> and then plotted using DRAWTREE from the PHYLIP package <sup>40</sup>. The structural comparisons are performed in Secondary-Structure Match SSM <sup>41</sup>.

## 2.3. Results and Discussion



### 2.3.1. Comparison with other monoheme cytochromes

There are a total of 14 small monoheme cytochromes (10–15 kDa) in *G. sulfurreducens*. However, a BLAST search with the sequence of PccH does not show any significant sequence homology with the other monoheme cytochromes from *G. sulfurreducens*. As reported previously<sup>35</sup>, the BLAST search revealed a relatively high homology (70% identity) with a monoheme c-type cytochrome from *Pelobacter propionicus* but modest homology with cytochromes from other organisms (**Figure 22**).



**Figure 22: Sequence alignment of the top six hits returned for the amino acid sequence of the mature PccH using the basic local alignment search tool (BLAST).** Pp, *P. propionicus*; Tn, *Thioalkalivibrio nitratireducens*; Ts, *Thioalkalivibrio sulfidophilus*; Lc, *Leptothrix cholodnii*; Rf, *Rhodoferrax ferrireducens*; P, *Polaromonas sp.* The sequence accession codes and the percentage identity with PccH are indicated. The conserved residues in the proteins are boxed: heme binding residues (gray) and other residues (black). Adapted from<sup>35</sup>.

Ambler's class I cytochromes include the subclasses of monoheme cytochromes  $c_2$ ,  $c_5$ ,  $c_6$ ,  $C_{551/552}$ ,  $C_{553}$  and  $C_{554}$ <sup>18,42</sup>. More recently, Stelter et al.<sup>43</sup> proposed a new subclass of class I cytochromes for c-type cytochromes from the bacteria of the Bacteroidetes phylum. Representative sequences from all the above mentioned cytochromes were used together with the top six hits returned for the BLAST search with PccH sequence to produce the dendrogram presented in **Figure 23**. From this analysis, it is clear that a separate group is formed by PccH and its most homologous sequences (**Figures 22** and **Figure 23**), suggesting that they are representatives of a new subclass within the class I cytochromes. Further structural evidence discussed below reinforces this proposal.

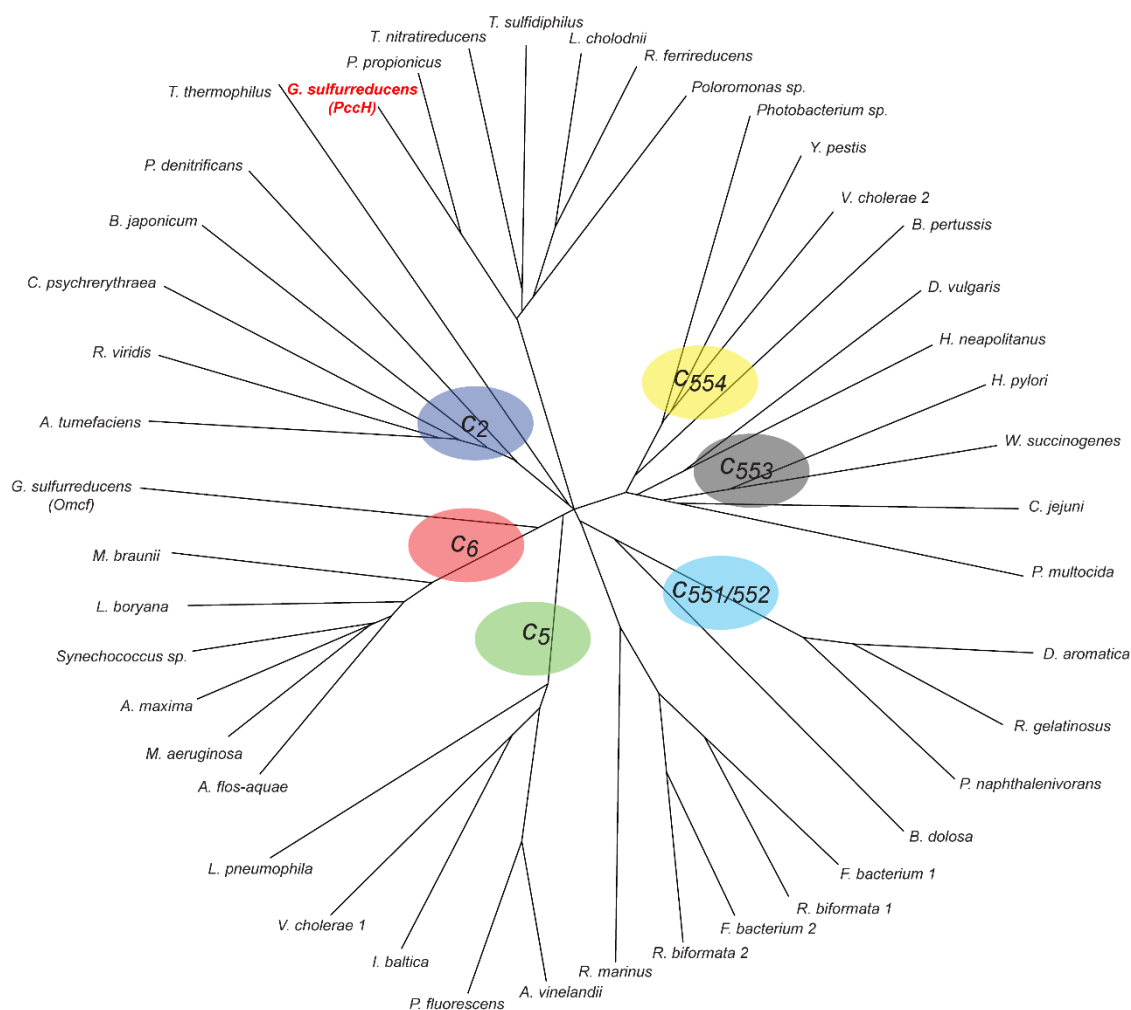


**Figure 23: Amino acid sequence comparison of Gs PccH cytochrome c with prokaryotic c-type monoheme cytochromes (accession number in parenthesis):** *Agrobacterium tumefaciens* (P00081); *Aphanizomenon flos-aquae* (P00116); *Arthrospira maxima* (P00118); *Azotobacter vinelandii* (AAC45922); *Bordetella pertussis* (Q7VVZ0); *Bradyrhizobium japonicum* (Q89SL2); *Burkholderia dolosa* (ZP\_00982883); *Campylobacter jejuni* (NP\_282300); *Colwellia psychrerythraea* (YP\_270114); *Dechloromonas aromatica* (AAZ45778); *Desulfovibrio vulgaris* (YP\_012252); *Flavobacteroides bacterium 1* (ZP\_01105921); *Flavobacteroides bacterium 2* (ZP\_01105294); *Gs PccH* (GSU3274); *Gs OmcF* (NP\_953478); *Halothiobacillus neapolitanus* (P25938); *Helicobacter pylori* (WP\_000756023.1); *Idiomarina baltica* (ZP\_01041945); *Legionella pneumophila* (YP\_096733); *Leptolyngbya boryana* (P00117); *Leptothrix cholodnii* (YP\_001792017.1); *Microcystis aeruginosa* (P00112); *Paracoccus denitrificans* (P00096); *Pasteurella multocida* (NC\_002663); *P. propionicus* (YP\_900515); *Photobacterium sp.* (ZP\_01162384); *Polaromonas sp.* (YP\_546929.1); *Polaromonas naphthalenivorans* (ZP\_01020507); *Pseudomonas fluorescens* (YP\_351250); *Rhodothermus marinus* (ACA83734.1); *Rhodopseudomonas viridis* (1CO6); *Robiginitalea biformata 1* (ZP\_01120248); *Robiginitalea biformata* (ZP\_01119795); *Rhodoferax ferrireducens* (YP\_521339.1); *Rubrivivax gelatinosus* (ZP\_00243317); *Synechococcus sp.* (P00115); *Thermus thermophilus* (1C52); *T. nitratireducens* (YP\_007216771.1); *T. sulfidophilus* (YP\_002512332.1); *Vibrio cholerae 1* (NP\_229825); *Vibrio cholerae 2* (NP\_231872); *Wolinella succinogenes* (NP\_906926); *Yersinia pestis* (CAC89905). The Ambler's class I monoheme cytochromes subclasses  $c_2$ ,  $c_5$ ,  $c_6$ ,  $c_{551/552}$ ,  $c_{553}$  and  $c_{554}$  are labeled. The two unlabeled groups correspond to the c-type cytochromes from the bacteria of the Bacteroidetes phylum and Gs PccH cytochrome (highlighted in red) and the top six hits returned for the BLAST search with PccH (Figure 24).

The proteins of the PcCH family contain the largest monoheme cytochromes observed to date, with ~ 129 amino acids. For comparison, the mitochondrial cytochromes have ~ 104 amino acids, whereas the other subclasses of class I cytochromes are even smaller (~ 80 amino acids). PcCH is structurally quite different from any of the other class I cytochromes.

Structural alignment with secondary structure matching<sup>41</sup> also did not reveal any significant structural homologs; cytochrome *c*<sub>554</sub> from *Chlorobaculum tepidum* (PDB code: 4J20) is the top hit in this search, with a Z-score of 2.7 (rmsd = 3.8 Å for 69 residues aligned) and 50% of sequence identity.

The structure of PcCH is unique among all the monoheme cytochromes of class I known to date<sup>18,42</sup>. For comparison, a gallery of structures of bacterial monoheme *c*-type cytochrome representatives from each of the subclasses is shown in **Figure 24**. There are a significant number of amino acids strictly conserved in the PcCH family of cytochromes (**Figure 22**). Thirty-four of 129 residues (29%), including the two cysteines and the axial ligands histidine and methionine residues, are conserved. Therefore, it is likely that the structural fold of this family of cytochromes will be conserved.

We propose that PcCH together with the cytochromes with similar sequences from other species (**Figure 22**) forms a new subclass within the class I cytochromes.

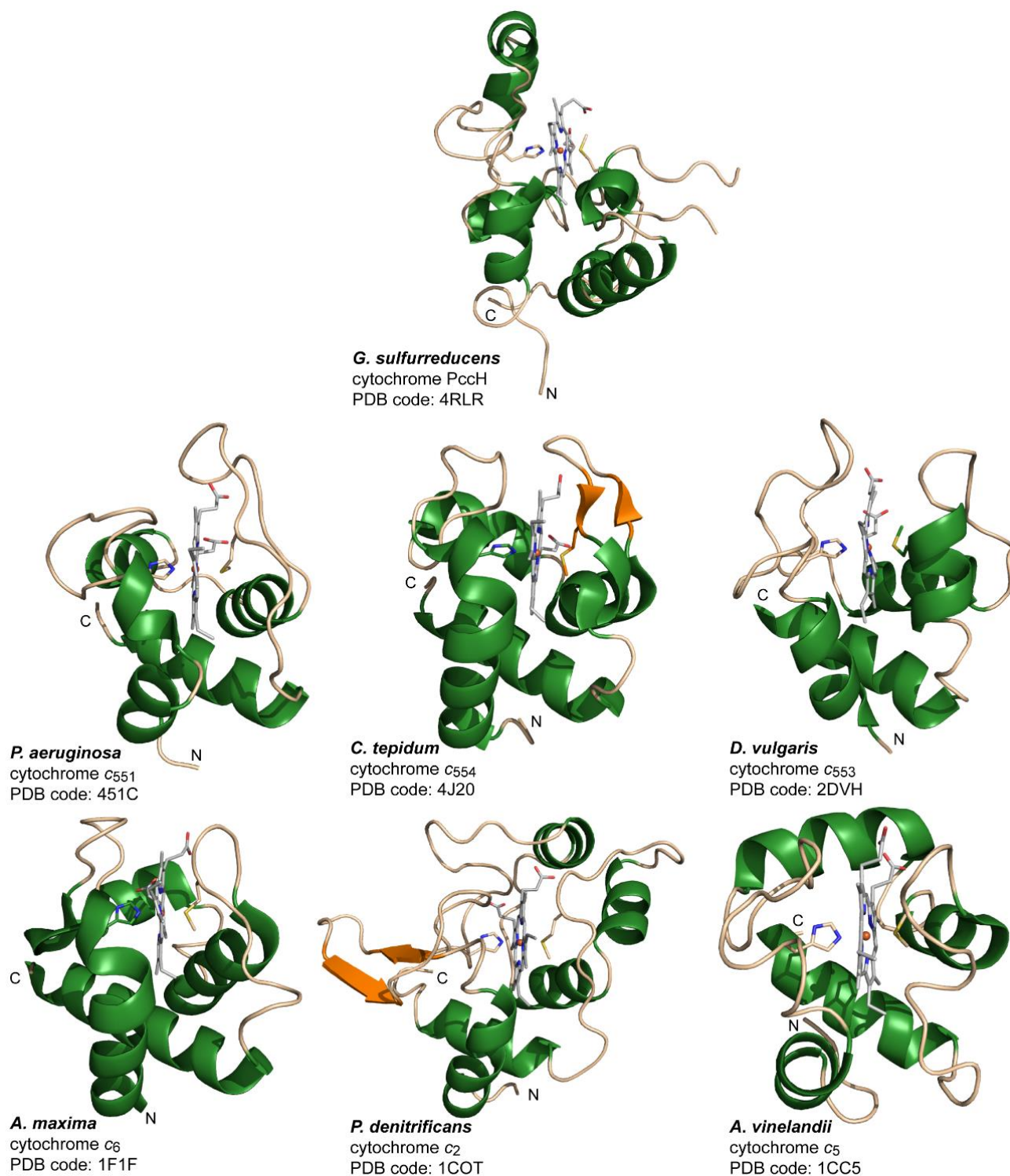
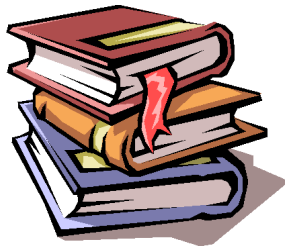


**Figure 24: A gallery of representative bacterial class I monoheme cytochromes including PcCH shown as cartoons.** The heme orientation is approximately the same in each case with the respective N- and C-termini labeled; the helical regions are shown in green,  $\beta$ -strands in orange and loops in light brown.





# 3. References



1. Lin, W. C., Coppi, M. V. and Lovley, D. R. *Geobacter sulfurreducens* Can Grow with Oxygen as a Terminal Electron Acceptor. *Appl. Environ. Microbiol.* 70, 2525–2528 (2004).
2. Röling, W. F. M., Breukelen, B. M. Van, Breukelen, B. M. V. a N. & Braster, M. Relationships between Microbial Community Structure and Hydrochemistry in a Landfill Leachate-Polluted Aquifer Relationships between Microbial Community Structure and Hydrochemistry in a Landfill Leachate-Polluted Aquifer. *Appl. Environ. Microbiol.* 67, 4619–4629 (2001).
3. Lin, B., Westerhoff, H. V & Röling, W. F. M. How *Geobacteraceae* may dominate subsurface biodegradation: physiology of *Geobacter metallireducens* in slow-growth habitat-simulating retentostats. *Environ. Microbiol.* 11, 2425–33 (2009).
4. Rooney-varga, J. N. *et al.* Microbial Communities Associated with Anaerobic Benzene Degradation in a Petroleum-Contaminated Aquifer Microbial Communities Associated with Anaerobic Benzene Degradation in a Petroleum-Contaminated Aquifer. 65, 3056–3063 (1999).
5. Sung, Y. *et al.* *Geobacter lovleyi*. *Society* 72, 2775–2782 (2006).
6. Ahrendt, A. J. *et al.* Steady state protein levels in *Geobacter metallireducens* grown with iron (III) citrate or nitrate as terminal electron acceptor. *Proteomics* 7, 4148–57 (2007).
7. Lovley, D. R. Electromicrobiology. *Annu. Rev. Microbiol.* 66, 391–409 (2012).
8. Geobacter project. at <<https://www.geobacter.org/>> (10/03/2015)
9. Coppi, M. V *et al.* Development of a Genetic System for *Geobacter sulfurreducens*. *Appl. Environ. Microbiol.* 67, 3180–3187 (2001).
10. Aklujkar, M. *et al.* The genome sequence of *Geobacter metallireducens*: features of metabolism, physiology and regulation common and dissimilar to *Geobacter sulfurreducens*. *BMC Microbiol.* 9, 109 (2009).
11. Juárez, J. F. *et al.* Identification of the *Geobacter metallireducens* bamVW two-component system, involved in transcriptional regulation of aromatic degradation. *Appl. Environ. Microbiol.* 76, 383–5 (2010).
12. Lovley, D. R. Microbial Energizers: Fuel Cells That Keep on Going. *Microbe* 1, 323–329 (2006).
13. Heintz, D. *et al.* Differential Membrane Proteome Analysis Reveals Novel Proteins Involved in the Degradation of Aromatic Compounds in *Geobacter metallireducens* 2159–2169 (2009).
14. Senko, J. M. and Stolz, J. F. Evidence for Iron-Dependent Nitrate Respiration in the Dissimilatory Iron-Reducing Bacterium *Geobacter metallireducens* Evidence for Iron-Dependent Nitrate Respiration in the Dissimilatory Iron-Reducing Bacterium *Geobacter metallireducens*. 4–7 (2001).
15. Tremblay, P.-L. *et al.* A genetic system for *Geobacter metallireducens*: role of the flagellin and pilin in the reduction of Fe(III) oxide. *Environ. Microbiol. Rep.* 4, 82–8 (2012).
16. Kashima, H. and Regan, J. M. Facultative Nitrate Reduction by Electrode-Respiring *Geobacter metallireducens* Biofilms as a Competitive Reaction to Electrode Reduction in a Bioelectrochemical System. *Environ. Sci. Technol.* 150209132002003 (2015).
17. Fonseca, B. M. *et al.* The role of intramolecular interactions in the functional control of multiheme cytochromes c. *FEBS Lett.* 586, 504–9 (2012).
18. Bertini, I., Cavallaro, G. and Rosato, A. Cytochrome c: Occurrence and Functions. 90–115 (2006).
19. Morgado, L. *et al.* One simple step in the identification of the cofactors signals, one giant leap for the solution structure determination of multiheme proteins. *Biochem. Biophys. Res. Commun.* 393, 466–470 (2010).

20. Morgado, L. *et al.* Fine Tuning of Redox Networks on Multiheme Cytochromes from *Geobacter sulfurreducens* Drives Physiological Electron/Proton Energy Transduction. *Bioinorg. Chem. Appl.* 2012, 298739 (2012).
21. Lloyd, J. R. *et al.* cytochrome in *Geobacter sulfurreducens*. 161, 153–161 (2003).
22. Morgado, L. *et al.* Thermodynamic characterization of a triheme cytochrome family From *Geobacter sulfurreducens* reveals mechanistic And functional diversity. *Biophys. J.* 99, 293–301 (2010).
23. Correia, I. J. *et al.* Thermodynamic and kinetic characterization of trihaem cytochrome  $c_3$  from *Desulfuromonas acetoxidans*. *Eur. J. Biochem.* 269, 5722–5730 (2002).
24. Pokkuluri, P. R. *et al.* Structural characterization of a family of cytochromes  $c_7$  involved in Fe(III) respiration by *Geobacter sulfurreducens*. *Biochim. Biophys. Acta - Bioenerg.* 1797, 222–232 (2010).
25. Shrestha, P. M. *et al.* Transcriptomic and genetic analysis of direct interspecies electron transfer. *Appl. Environ. Microbiol.* 79, 2397–2404 (2013).
26. Altschul, S. *et al.* Gapped BLAST and PSI- BLAST: a new generation of protein database search programs. *Nucleic acids Res* 25, 3389–3402 (1997).
27. Petersen, T. N. *et al.* SignalP 4.0: discriminating signal peptides from transmembrane regions. *Nat. Methods* 8, 785–6 (2011).
28. Rose, R. E. The nucleotide sequence of pACYC184. *Nucleic acids Res* 16, 355 (1988).
29. Arslan, E. *et al.* Overproduction of the Bradyrhizobium japonicum  $c$ -Type Cytochrome Subunits of the  $cbb$  3 Oxidase in *Escherichia coli*. *Biochemical and Biophysical research communications* 251, 744–747 (1998).
30. Londer, Y. Y. *et al.* Production and preliminary characterization of a recombinant triheme cytochrome  $c_7$  from *Geobacter sulfurreducens* in *Escherichia coli*. *Biochim. Biophys. Acta - Bioenerg.* 1554, 202–211 (2002).
31. Gasteiger, E. *et al.* Protein Identification and Analysis Tools on the ExPASy Server. 571–608 (2005). at <[http://web.expasy.org/docs/expasy\\_tools05.pdf](http://web.expasy.org/docs/expasy_tools05.pdf)> 21/10/2014
32. Downing, a. K. *Protein NMR Techniques.* 278, (2004).
33. Fernandes, A. P. *et al.* Isotopic labeling of  $c$ -type multiheme cytochromes overexpressed in *E. coli*. *Protein Expr. Purif.* 59, 182–8 (2008).
34. Pierattelli, R., Banci, L. and Turner, D. L. Indirect determination of magnetic susceptibility tensors in peroxidases: a novel approach to structure elucidation by NMR. *JBIC* 320–329 (1996).
35. Dantas, J. M. *et al.* Functional characterization of P $c$ H, a key cytochrome for electron transfer from electrodes to the bacterium *Geobacter sulfurreducens*. *FEBS Lett.* 587, 2662–8 (2013).
36. Ross, D. E. *et al.* Towards electrosynthesis in *Shewanella*: Energetics of reversing the Mtr pathway for reductive metabolism. *PLoS One* 6, (2011).
37. Shrestha, P. M. *et al.* Transcriptomic and genetic analysis of direct interspecies electron transfer. *Appl. Environ. Microbiol.* 79, 2397–404 (2013).
38. McGinnis, S. and Madden, T. L. BLAST: at the core of a powerful and diverse set of sequence analysis tools. *Nucleic Acids Res.* 32, W20–5 (2004).
39. Larkin, M. A. *et al.* Clustal W and Clustal X version 2.0. *Bioinformatics* 23, 2947–8 (2007). 22/09/2014
40. Felsenstein, J. Phylogeny Inference Package (Version 3.2). 164–166 (1989). at <<http://evolution.genetics.washington.edu/phyip.html>> 22/09/2014
41. Krissinel, E. and Henrick, K. Secondary-structure matching (SSM), a new tool for fast protein structure alignment in three dimensions. *Acta Crystallogr. Sect. D Biol. Crystallogr.* 60, 2256–2268 (2004).

42. Ambler, R. P. Sequence variability in bacterial cytochromes c. *Biochim. Biophys. Acta - Bioenerg.* 1058, 42–47 (1991).
43. Meike Stelter *et al.* Novel Type of Monoheme Cytochrome c: Biochemical and Structural Characterization. *Biochemistry* 47, 11953–11963 (2008).

## 4. Supplementary





## **4.1. Cloning**





```

      1       10       20       30       40       50       60
      |       |       |       |       |       |       |
ppcE  A A T T C A T G A T A C A G C C A A A G G A C T C T C G T C A T G A A A A G G A C C G T A C C C C T G C T G A T T G T T
FW    - - - - -
RV    - - - - -

ppcE  T T G A T G G T T A A C G T A C C C G T C G T C A A G G C T G C G G A T A C C A T G A T A T T C C G G C A A A A A C
FW    - - - - - C G T A C C C G T C G C G G C C G C T G C G G A T A C C A T G A T A T T C - - - - -
RV    - - - - -

ppcE  G G A A A T A T T A C C T T T A A T C A C A A A C A C C A C A C G G A T C T C C T C A A G G A A T G C A A G A A C T G T
FW    - - - - -
RV    - - - - -

ppcE  C A C G A C A A A A C C C C T G G A A G A A T T G C C A A T T T C G G C A A A G A C T A C G C T C A T A A G A C C T G C
FW    - - - - -
RV    - - - - -

ppcE  A A G G G A T G C C A C G A G G T G A G G G G A A C T G G G C C A A C G C G C T G C G G C C T C T G C C A C A G G A A G
FW    - - - - -
RV    - - - - - G C C A C A G G A A G

ppcE  T A G C A C C C T T G A T G T C A T A A A A A G C C G G T T T C C
FW    - - - - -
RV    T A G C A C C C T T G A T G T C A A G C T T A G C C G G - - - - -

```

**Figure A- 3: Sequence of ppcE and the primers forward (FW) and reverse (RV) used for the gene amplification.** The restriction sites for the enzymes *NotI* and *HindIII* are indicated in orange and purple, respectively.

```

      1       10       20       30       40       50       60
      |       |       |       |       |       |       |
ppcF  C A G G C A T C T A A C C A A C A A A A G G A G A A C A A T G T G A A A A A A A C A G C T A T C A C C A T C G C C T T C
FW    - - - - -
RV    - - - - -

ppcF  G T C G C C A C T T C T G C C T T T G C C G C A C A T G T T T T C G C C G C C G A C G T A T T T G A A T T C C C C G C A
FW    - - - - - C A C A T G C G G C C G C C G C C G A C G T A T T T G A A T T C - - - - -
RV    - - - - -

ppcF  T C A A T G G G T A A A G T G A C A T T C C C C A T A A A A T G C A C C A G G A G A T G C T G A A G G A C T G C A A G
FW    - - - - -
RV    - - - - -

ppcF  A A G T G C C A C G A A A A C G G A C C G G G C A A G A T C A A G G A C T T C G G C A A G G A C T G G G C C C A C A A G
FW    - - - - -
RV    - - - - -

ppcF  A C C T G C A A G G G G T G C C A T A C C G A G C T G A A G A A A G G C C C G G T C G G C T G C A C G G A C T G C C A C
FW    - - - - -
RV    - - - - - C T G C C A C

ppcF  A A G A A G T A A A T A T G G G A A C C T G C G G T A G G G G C G C T G C T T
FW    - - - - -
RV    A A G A A G T A A A A G C T T G A A C C T G C G G T A G G G G C - - - - -

```

**Figure A- 4: Sequence of ppcF and the primers forward (FW) and reverse (RV) used for the gene amplification.** The restriction sites for the enzymes *NotI* and *HindIII* are indicated in orange and purple, respectively.

## B. PCR programs

**Table B- 1: PHUSION program**

| <b>Cycle</b> | <b>Temperature</b> | <b>Time</b>    |
|--------------|--------------------|----------------|
| 1            | 98°C               | 30s            |
| 2            | 98°C               | 7s             |
| 3            | 72°C               | 40s 34(cycles) |
| 4            | 72°C               | 10 min         |

**Table B- 2 : PCR colonies program**

| <b>Cycle</b> | <b>Temperature</b> | <b>Time</b>    |
|--------------|--------------------|----------------|
| 1            | 95°C               | 5 min          |
| 2            | 95°C               | 30 s           |
| 3            | 55°C               | 30s            |
| 4            | 72°C               | 60s 34(cycles) |
| 5            | 72°C               | 10 min         |

### C. Gel electrophoresis

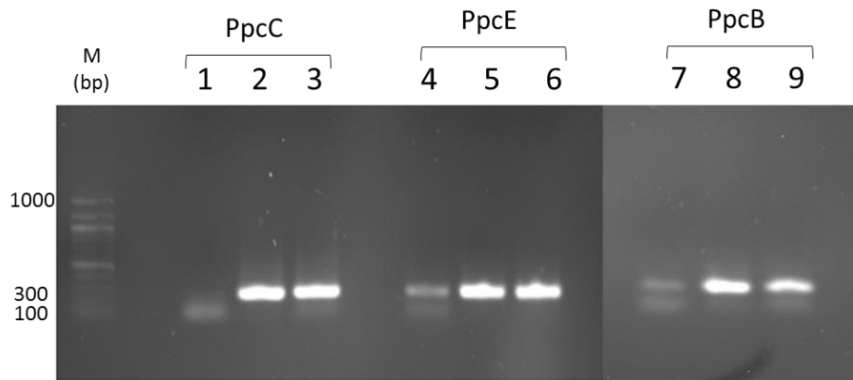


**Figure C- 1: Agarose gel electrophoresis (0.8%) with the result of PCR fragment amplification for ppcC (351 bp), ppcE (336 bp), ppcB (336 bp). Gene ruler 100 bp DNA ladder (M). For each protein one negative control (without DNA) and two PCR fragment amplified.**

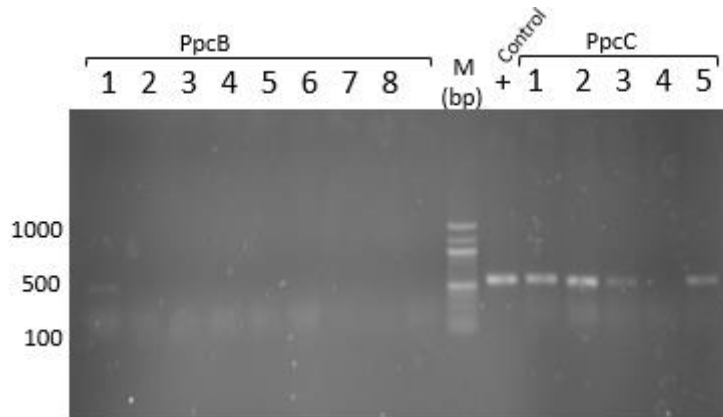


**Figure C- 2: Agarose gel electrophoresis (0.8%) with the result of colonies PCR amplification with pCK32 primers for PpcB and PpcC. From the left to the right: PCR fragment amplified corresponding to PpcB (1,2...8); gene ruler 100 bp DNA ladder (M), positive control; PCR fragment amplified corresponding to PpcC using a ligation ratio 5:1 (vector:fragment) (1,2,...5).**

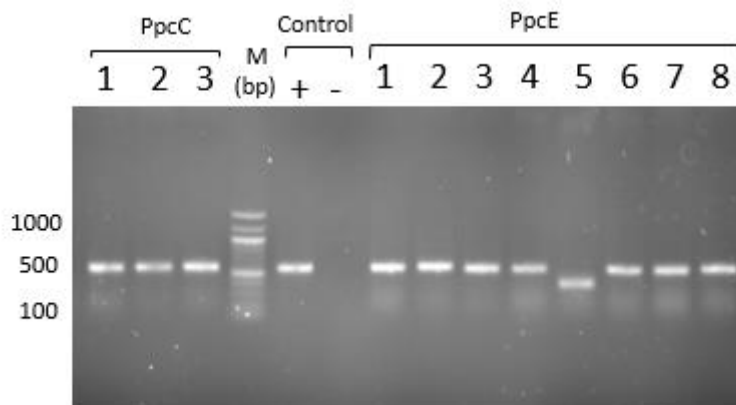


**Figure C- 3: Agarose gel electrophoresis (0.8%) with the result of colonies PCR amplification with pCK32 primers for PpcC and PpcE. From the left to the right: PCR fragment amplified corresponding to PpcC using a ligation ratio 3:1 (vector:fragment) (1,2,3), gene ruler 100 bp DNA ladder (M); positive control; negative control; PCR fragment amplified corresponding to PpcE (1,2...8).**

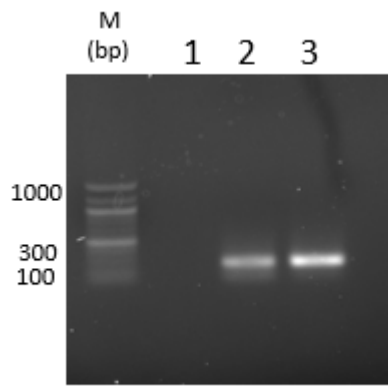


**Figure C- 4:Agarose gel electrophoresis (0.8%) with the result of PCR fragment amplification for ppcB (336 bp) with a different cloning protocol described in section 1.3.1.. From the left to the right: gene ruler 100 bp DNA ladder (M), one negative control (without DNA) and two PCR fragment amplified.**

## D. DNA Sequencing Results

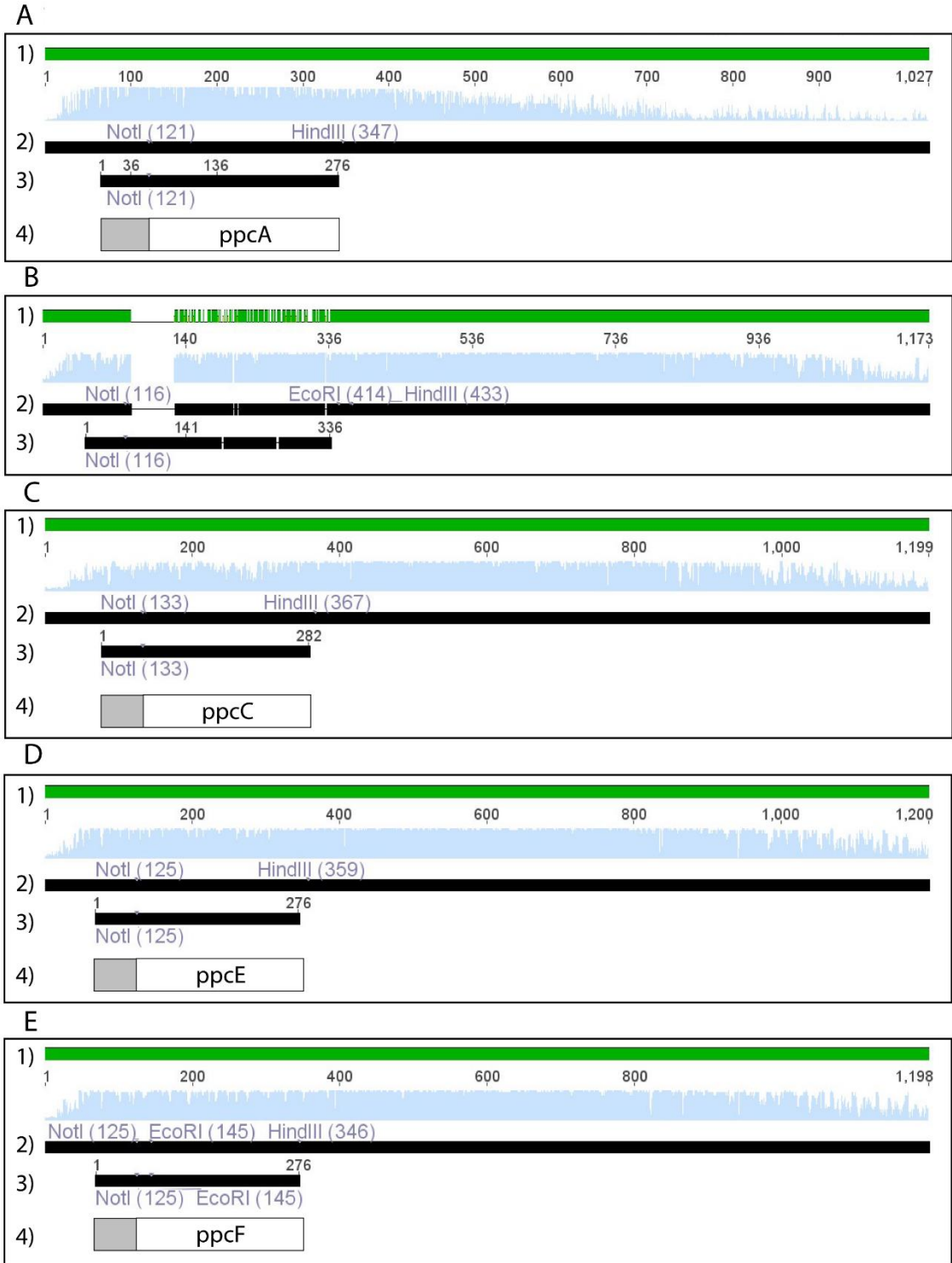


**Figure D- 1: DNA sequencing results for each  $\alpha$ -type cytochrome from *G. metallireducens*. 1) Alignment of the sequencing product with the gene sequence. 2) Sequencing product. 3) OmpA sequence with gene sequence. 4) OmpA sequence (grey bar) with gene sequence (white bar).**



## **4.2. Purification**

### E. PpcF purification steps

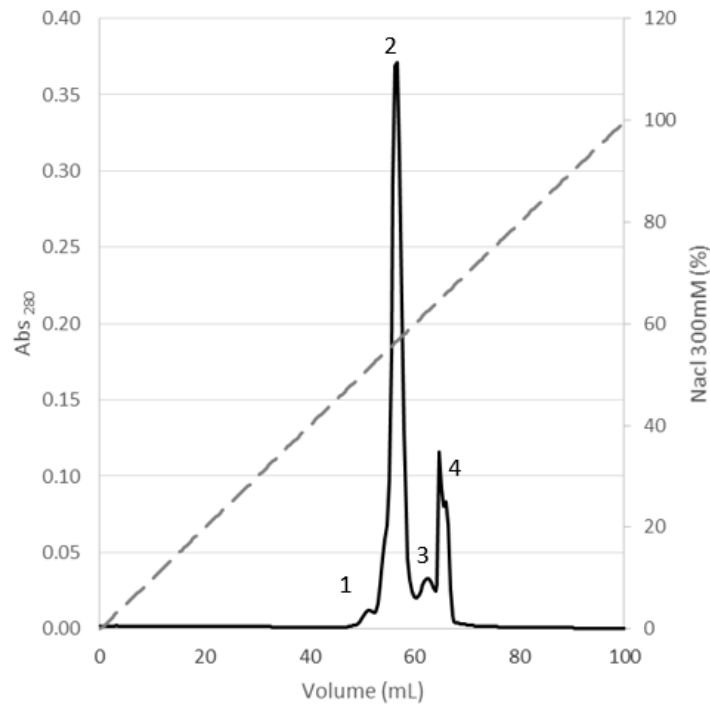


**Figure E- 1: Elution profile for the cation exchange column chromatography equilibrated with 10 mM Tris-HCl, pH 7.5 for PpcF (flow rate of 1 ml/min).** Primary and second y-axis, represent the variation of the absorbance at 280 nm (dark solid line) and the NaCl gradient profile (grey dashed line), respectively.

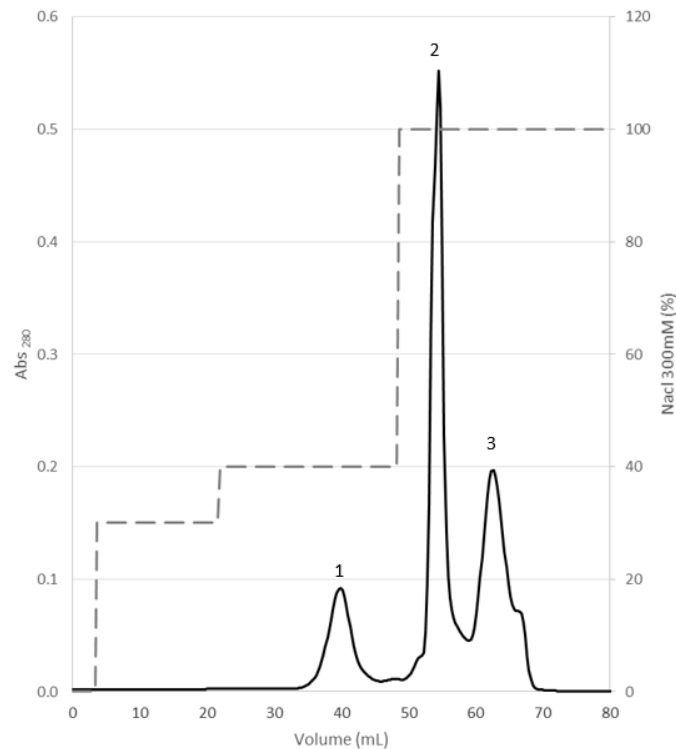


**Figure E- 2: Elution profile for the cation exchange column chromatography equilibrated with 10 mM Tris-HCl, pH 8.5 for PpcF (flow rate of 1 ml/min).** Primary and second y-axis, represent the variation of absorbance at 280 nm (dark solid line) and the stepwise elution with 30%, 40% and 100% of the NaCl gradient (grey dashed line), respectively.



## F. Purification of PpcC

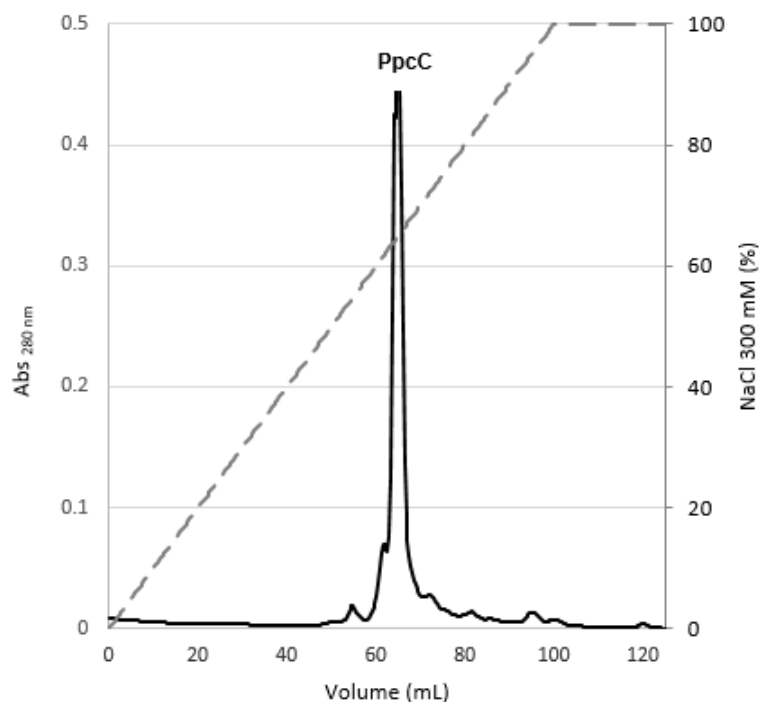


**Figure F- 1:** Elution profile for the cation exchange column chromatography equilibrated with 10 mM Tris-HCl, pH 8 for PpcC (flow rate of 1 ml/min). Primary and second y-axis, represent the variation of absorbance at 280 nm (dark solid line) and the NaCl gradient profile (grey dashed line), respectively. The

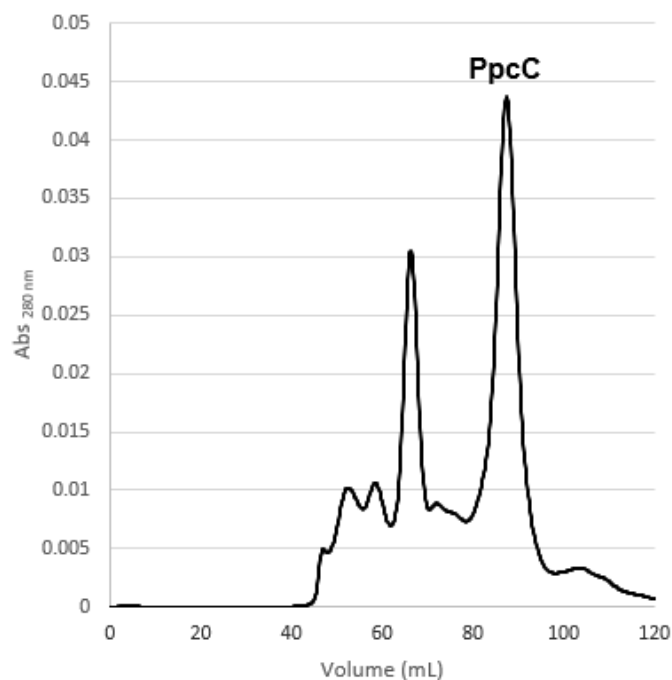


**Figure F- 2:** Elution profile for the molecular exclusion column chromatography equilibrated with 100 mM sodium phosphate buffer, pH 8 for PpcC. The red fractions correspondent to PpcC eluted at 85 ml.

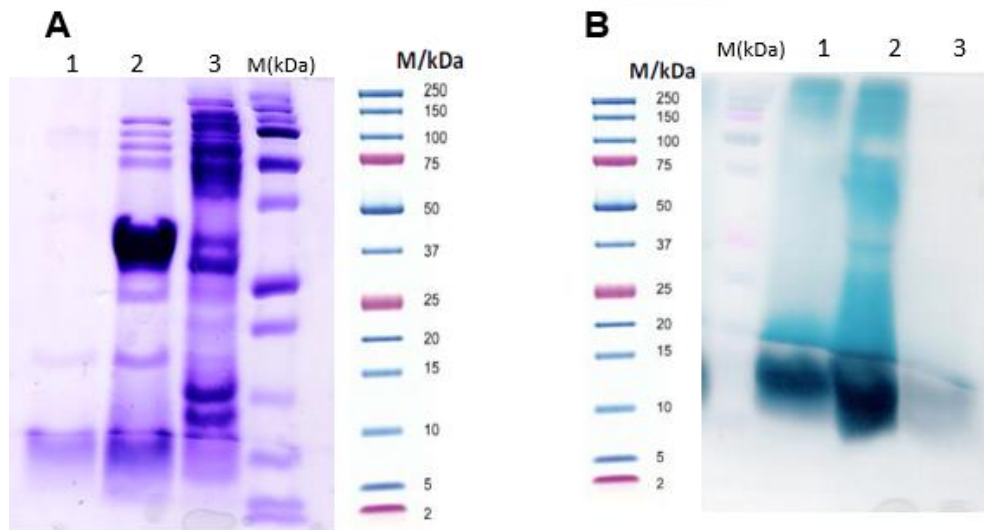


**Figure F- 3: SDS-PAGE electrophoresis gel stained with Coomassie blue (A) and the TMBZ/H<sub>2</sub>O<sub>2</sub> (B) correspondent to the collected fractions of PpcC cytochrome purification steps. From the left to the right: 1- molecular exclusion column chromatography, 2- cation exchange column chromatography, 3- periplasmic fraction and marker Precision plus protein<sup>™</sup> Dual Xtra Standards (M).**

### G. Purification of PpcE

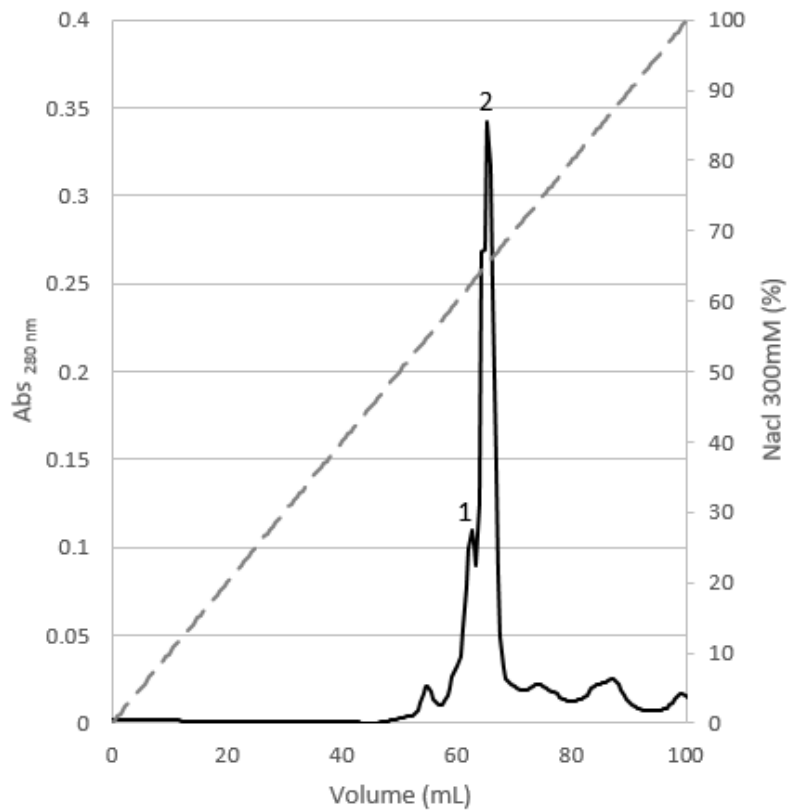


**Figure G- 1: Elution profile for the cation exchange column chromatography equilibrated with 10 mM Tris-HCl, pH 8 for PpcE (flow rate of 1 ml/min).** Primary and second y-axis, represent the variation of absorbance at 280 nm (dark solid line) and the NaCl gradient profile (grey dashed line), respectively. Two bands (1 and 2) are collected as indicated in the profile of elution.

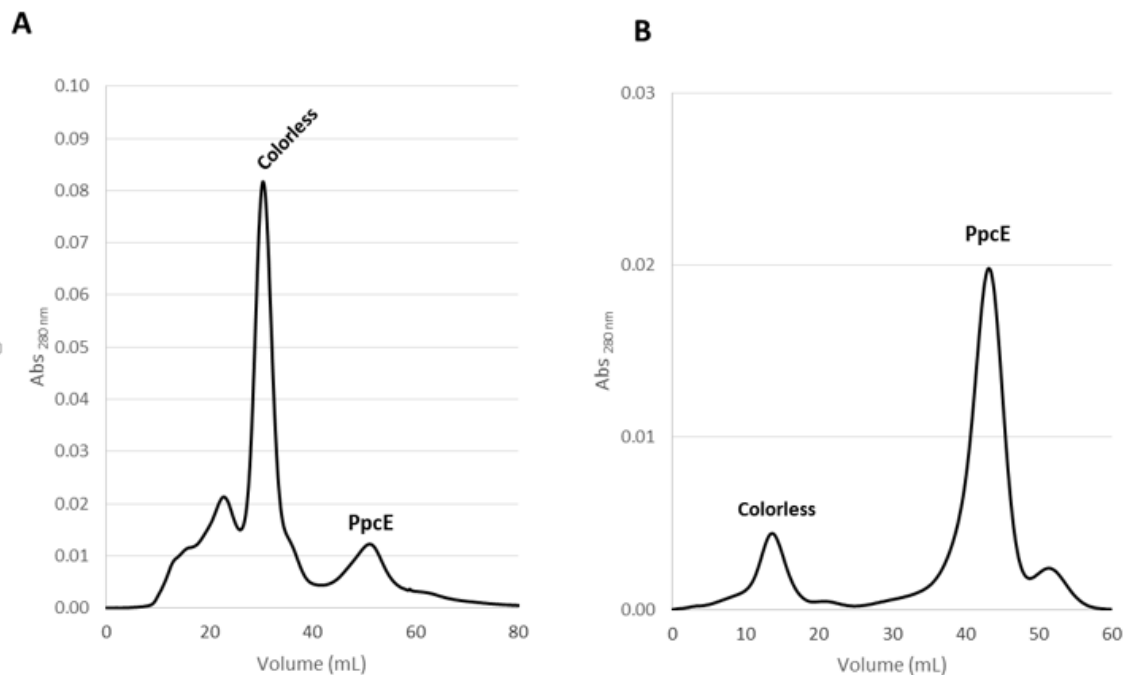


**Figure G- 2: Elution profiles for the molecular exclusion column chromatography equilibrated with 100 mM sodium phosphate buffer, pH 8 for PpcE.** A- Corresponding to the fractions of band 1 of cation

exchange chromatography; B- Corresponding to the fractions of band 2 of cation exchange chromatography.

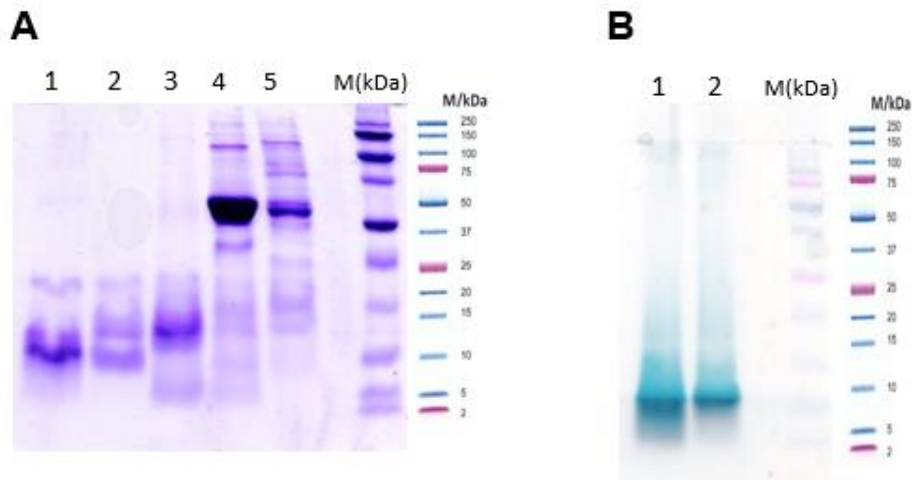


**Figure G- 3: SDS-PAGE electrophoresis gel stained with Coomassie blue (A) and the TMBZ/H<sub>2</sub>O<sub>2</sub> (B) correspondent to the collected fractions of PpCE cytochrome purification steps. From the left to the right: 1- molecular exclusion column chromatography (band 1); 2- molecular exclusion column chromatography (band 2); 3- cation exchange column chromatography (band 2); 4- cation exchange column chromatography (band 1); 5- periplasmic fraction and marker Precision plus protein™ Dual Xtra Standards (M).**

## H. Resume of Purification

**Table H- 1** Calculated molecular weight and isoelectric point for the triheme cytochromes from *G. metallireducens* using the EXPASY tool<sup>31</sup>

| Protein     | pI   | Molecular weight (Da)* |
|-------------|------|------------------------|
| <b>PpcA</b> | 9.32 | 9681.08                |
| <b>PpcB</b> | 9.39 | 9394.64                |
| <b>PpcC</b> | 8.86 | 9513.83                |
| <b>PpcE</b> | 9.36 | 9709.01                |
| <b>PpcF</b> | 8.96 | 9734.21                |

\* Total molecular mass considering a MW of 616 Da per heme.

**Table H- 2:** Elution gradient value and elution volume for the triheme cytochromes from *G. metallireducens* in the cationic and molecular exclusion chromatography steps, respectively.

| Protein     | Gradient value (%) <sup>1</sup> | Elution volume (ml) <sup>2</sup> |
|-------------|---------------------------------|----------------------------------|
| <b>PpcA</b> | 74                              | 85                               |
| <b>PpcB</b> | -                               | -                                |
| <b>PpcC</b> | 62                              | 85                               |
| <b>PpcE</b> | 65                              | 45                               |
| <b>PpcF</b> | 55; 65; 70; 75                  | 85                               |

<sup>1</sup> Gradient from 0 to 300 mM NaCl

<sup>2</sup> 16/60 superdex 75 gel column



## **4.3. Spectrometry and Spectroscopic Characterization**

## I. Mass spectrometry spectra

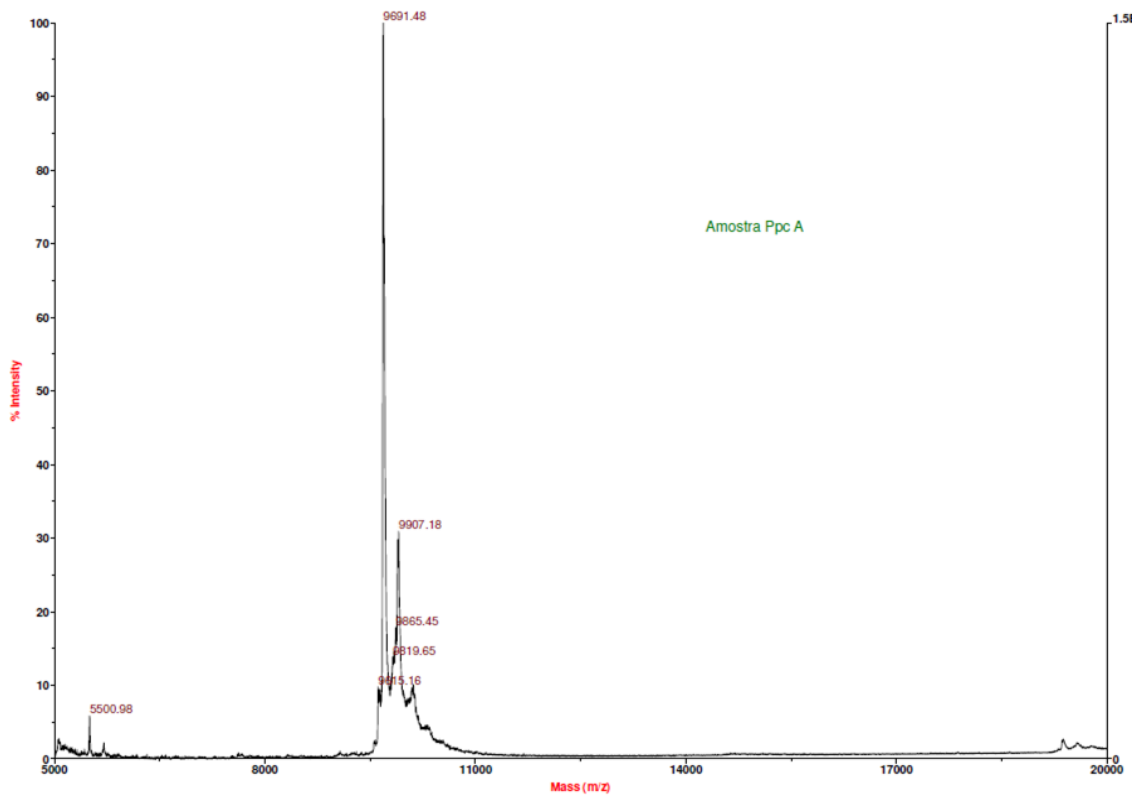


Figure I- 1 Mass spectrometry spectrum of purified PpcA. MALDI-TOF-MS with external calibration of horse cytochrome.

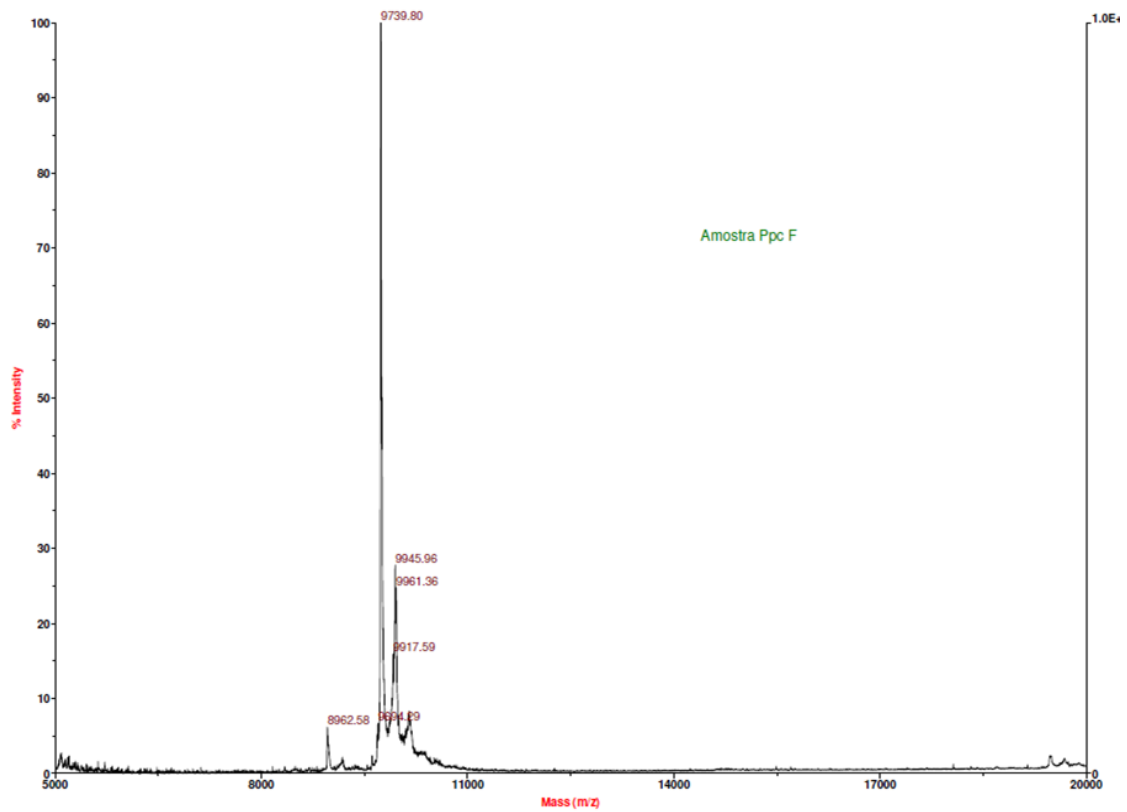


Figure I- 2: Mass spectrometry spectrum of purified PpcF. MALDI-TOF-MS with external calibration of horse cytochrome



## J. Visible spectra

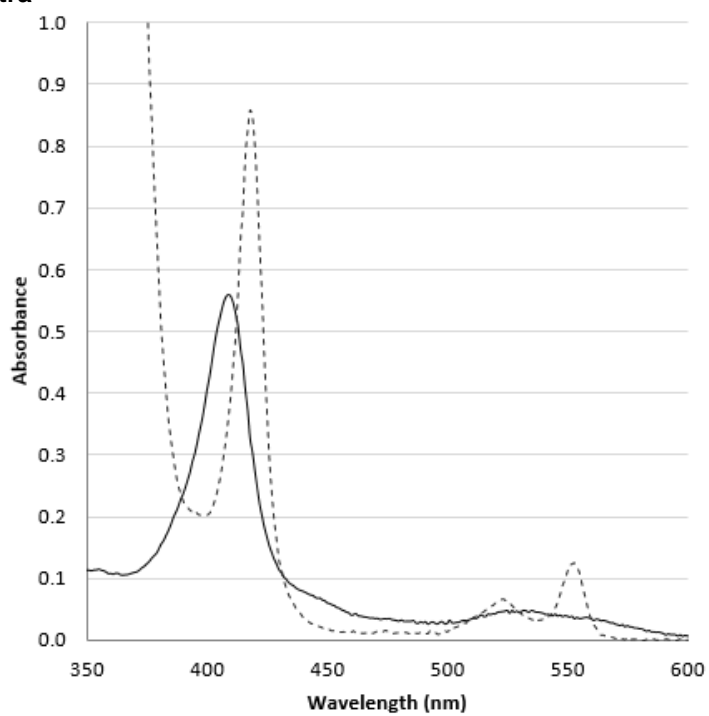


Figure J- 1: Absorption spectrum of PpcF in the oxidized (solid line) and reduced (dashed line).

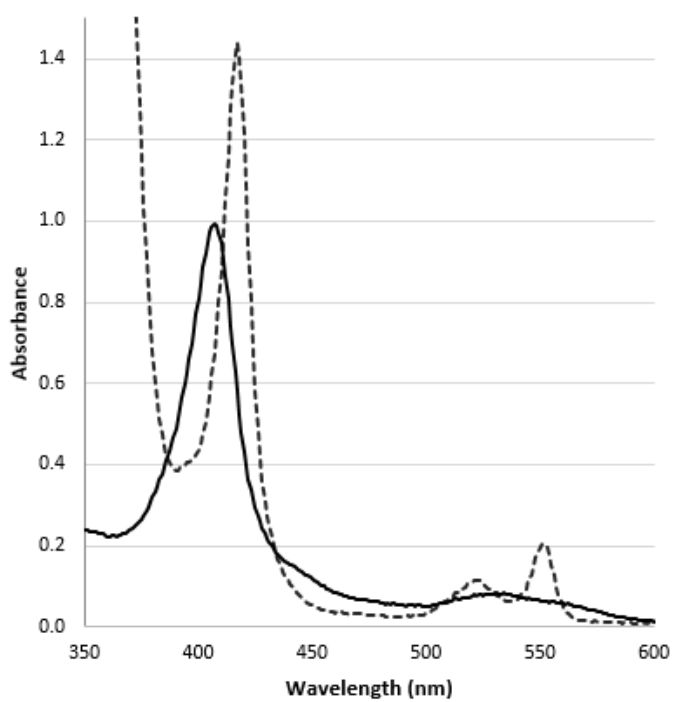


Figure J- 2: Absorption spectrum of PpcC in the oxidized (solid line) and reduced (dashed line).

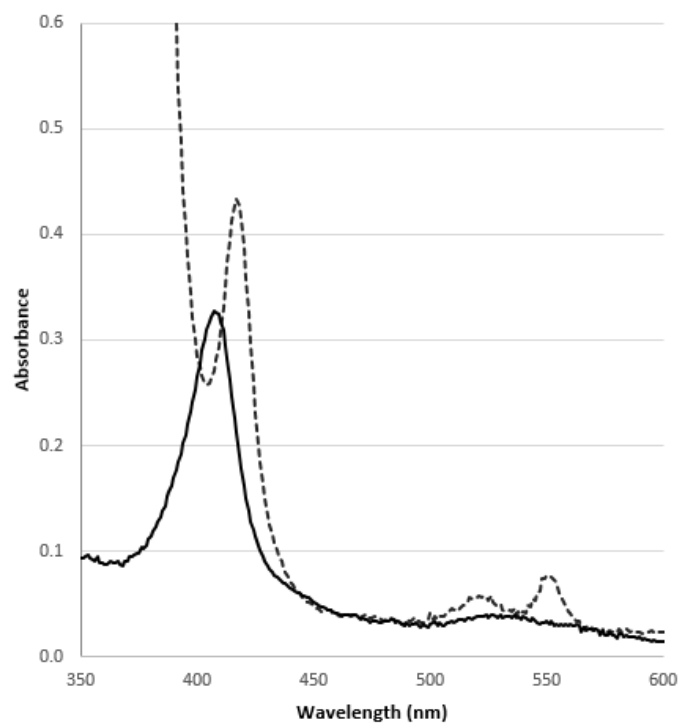


Figure J- 3: Absorption spectrum of PpCE in the oxidized (solid line) and reduced (dashed line).

## K. NMR spectra

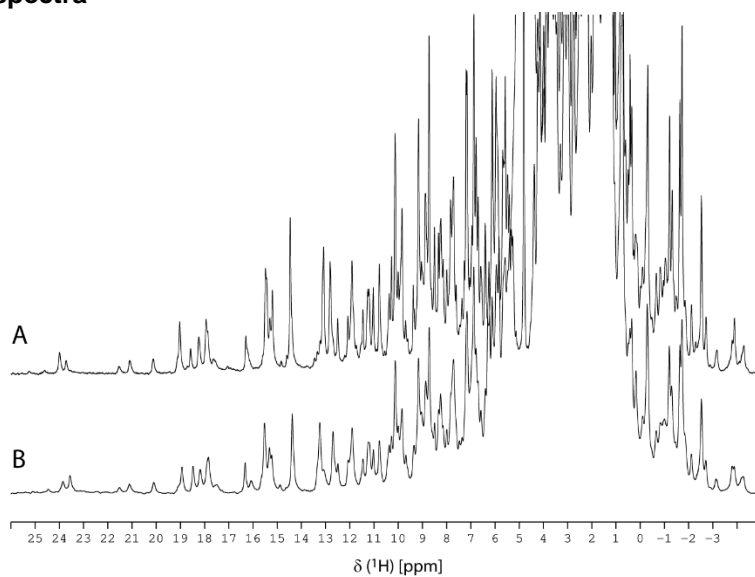


Figure K- 1:  $1D-^1H$  NMR spectra of the oxidized before (A) and after (B) lyophilized triheme cytochrome PpcF ( $70 \mu M$ ) obtained at  $25^\circ C$ .

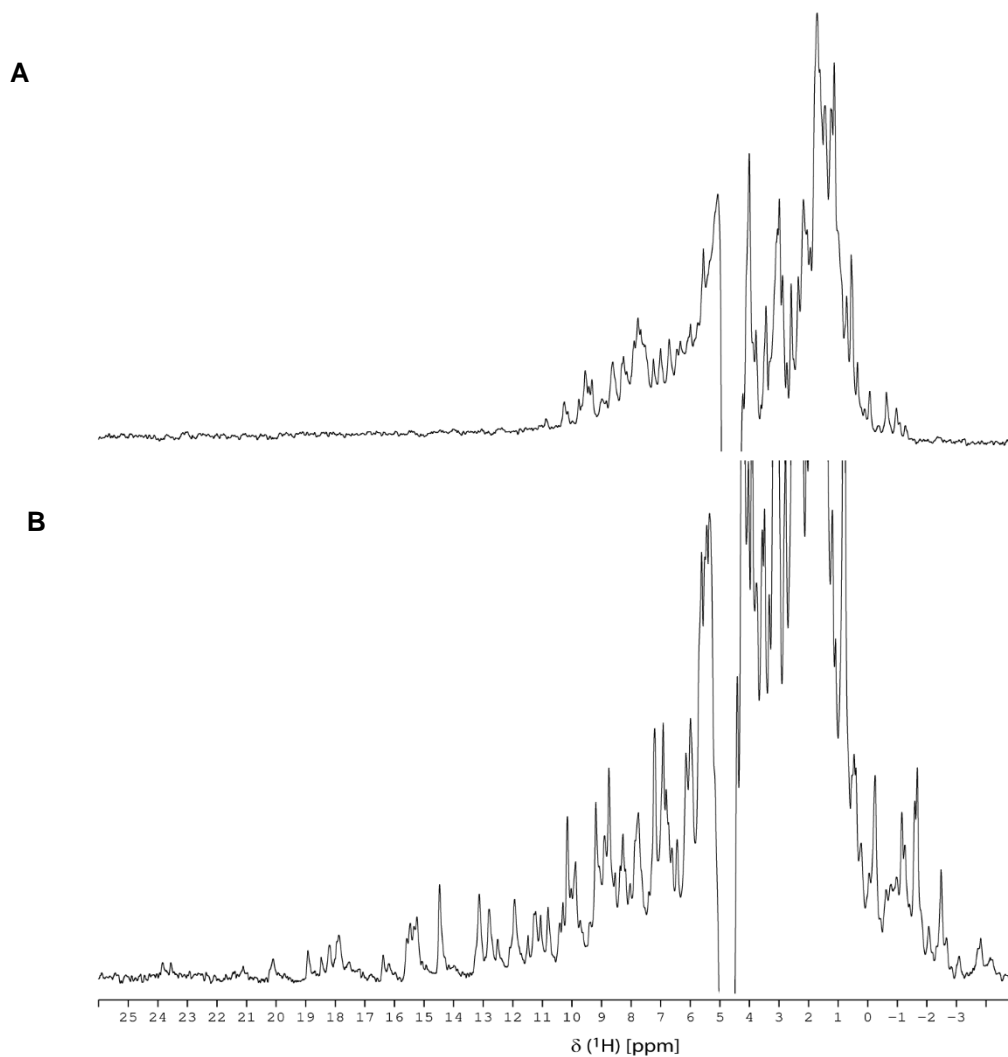


Figure K- 2:  $1D-^1H$  NMR spectra of the reduced (A) and oxidized (B) triheme cytochrome PpcF ( $70 \mu M$ ) obtained at  $25^\circ C$ .

## L. Solutions

Table L- 1: Main solutions used in this work

| Buffer   | Composition   | Quantity |
|--|---|----------|
| <b>LB medium solid</b><br>V=1 L                            | Peptone (Fluka)                                     | 10g      |
|  | Yeast extract (Himedia)                             | 5g       |
|  | NaCl(Panreac)                                       | 10g      |
| <b>2xYT medium solid</b><br>V=1 L                          | Peptone (Fluka)                                     | 16g      |
|  | Yeast extract (Himedia)                             | 10g      |
|  | NaCl(Panreac)                                       | 5g       |
| <b>LB medium solid</b><br>V=200 mL                         | Peptone (Fluka)                                     | 2g       |
|  | Yeast extract (Himedia)                             | 1g       |
|  | NaCl(Panreac)                                       | 2g       |
|  | Agar (nzytech)                                      | 4g       |
| <b>2xYT medium solid</b><br>V=200 mL                       | Peptone (Fluka)                                     | 3.2g     |
|  | yeast extract (Himedia)                             | 2g       |
|  | NaCl(Panreac)                                       | 1g       |
|  | Agar (nzytech)                                      | 3g       |
| <b>Lysis buffer</b><br>V=60mL                              | 20% sucrose (Fisher scientific)                     | 12g      |
|  | 1 M Tris-HCl (VWR chemicals) pH 8.0                 | 12mL     |
|  | 0.5 M EDTA pH 8 (Sigma)                             | 24 µL    |
| <b>1 M Tris-HCl pH8</b><br>V=1L                            | Tris (VWR chemicals)                                |          |
|  | Set pH 8 using HCl (Carlo Erba)                     | 121.14g  |
| <b>100 mM NaPi pH8</b><br>V=1L                             | 16.856 g Na <sub>2</sub> HPO <sub>4</sub> (Panreac) | 16.856   |
|  | 0.731 g NaH <sub>2</sub> PO <sub>4</sub> (Panreac)  | 0.731g   |
| <b>Loading Buffer SDS page</b><br>V=5 mL                   | 100 mM Tris HCl pH 6.8                              | 1 mL     |
|  | 20% glycerol (Fluka)                                | 2 mL     |
|  | 4% SDS (Fluka)                                      | 4g       |
|  | 200mM Mercaptoethanol                               | 140.5 µl |
| <b>Tris-glycine Buffer pH 8.3</b><br>V=1L                  | Tris (VWR chemicals)                                | 15.1g    |
|  | Glycine (nzytech)                                   | 72.05g   |
|  | 10% SDS (Fluka)                                     | 50 mL    |
| <b>SDS PAGE electrophoresis</b><br><b>Concentration 5%</b> | Solução II  | 450 µl   |
|  | Acrilamide/Bis (Fluka)                              | 300 µl   |
|  | H <sub>2</sub> O                                    |          |
|  | 10% PSA (Riedel-de Haën)                            | 1,020 mL |
|  | TEMED (Fluka)                                       | 13.5 µl  |
| <b>SDS PAGE electrophoresis</b><br><b>Resolution 15%</b>   | Solução I   | 750 µl   |
|  | Acrilamyde/Bis (Fluka)                              | 2.5 mL   |
|  | H <sub>2</sub> O                                    | 1,66 mL  |
|  | 10% PSA (Riedel-de Haën)                            | 38 µl    |
|  | TEMED (Fluka)                                       | 2.5 µl   |
| <b>Dye solution</b><br>V=1L                                | Blue comassie (Merck)                               | 1g       |
|  | Acetic acid (Sigma alderich)                        | 100 mL   |
|  | Methanol (Carlo Erba)                               | 400 mL   |
| <b>Bleach solution</b><br>V=1L                             | Acetic acid (Sigma alderich)                        | 100 mL   |
|  | Methanol (Carlo Erba)                               | 400 mL   |

**Table L- 2: Heme dye solution protocol**

| <b>Solution</b> | <b>Reagents</b>                   | <b>Preparation</b>   |
|-----------------|-----------------------------------|--|
| <b>A</b>        | 4,17mM TMBZ (Acrós organics)      | 30mg TMBZ in 30mL metanol (Carlo Erba). Protect from light |
| <b>B</b>        | 0,25M de Sodium acetate (Panreac) | 17,01g Sodium acetate in 500mL. Adjust pH to 5             |
| <b>C</b>        | Dye solution                      | Add 30mL solution A to 70mL solution B                     |
| <b>D</b>        | Wash solution                     | Mix 70mL solution B in 30mL propanol (Fluka)               |

Transfer the gel of acrylamide to dye solution (solution C), and maintain per 30 minutes protect from light and agitate. Add 300 µl 30% H<sub>2</sub>O<sub>2</sub> (Sigma Aldrich) and shake per 30 minutes. Wash two times with solution D.